Modern Stochastics: Theory and Applications 0 (0) (2026) 1–33
https://doi.org/10.15559/26-VMSTA305

Convergence rates for Euler schemes of Lévy-driven SDE using dynamic cutting

Victoria Knopova[a,b], **Denis Platonov**[a]

[a] *Taras Shevchenko National University of Kyiv, 01601 Kyiv, Ukraine*
[b] *Institute of Mathematics, National Academy of Sciences of Ukraine, 01024 Kyiv-4, Tereshchenkivska 3, Ukraine*

vicknopova@knu.ua (V. Knopova), vicknopova@imath.kiev.ua (V. Knopova), dplatonov@knu.ua (D. Platonov)

Received: 21 April 2025, Revised: 27 July 2026, Accepted: 27 July 2026,
Published online: 20 August 2026

Abstract We introduce a *dynamic cutting* approach for the numerical approximation of Lévy-driven stochastic differential equations. The key idea is to remove small jumps according to a time-dependent threshold, so that the retained jumps form a time-inhomogeneous compound Poisson process. We derive L^p-strong convergence rates for the adjusted Euler scheme. Numerical experiments at matched computational cost compare the dynamic cutting scheme with the classical Asmussen–Rosiński truncation and demonstrate consistently smaller strong errors when the time-dependent jump coefficient has a singularity at $t = 0$.

Keywords Lévy-driven SDE, Euler-Maruyama scheme, dynamic cutting
2020 MSC 60H10, 60H35, 60G51

1 Introduction

On a probability space $(\Omega, \mathcal{F}, \mathbb{P})$ consider a Brownian motion $(B_t)_{t\geq 0}$ and a Lévy process $(Z_t)_{t\geq 0}$, independent of $(B_t)_{t\geq 0}$. We assume that both processes are one-dimensional and with the same state space. We denote by $(\mathcal{F}_t)_{t\geq 0}$ the augmented filtration, generated by the Brownian motion $(B_t)_{t\geq 0}$ and $(Z_t)_{t\geq 0}$. Denote by $N(dt, dz)$ the Poisson random measure on $[0, \infty) \times \mathbb{R}$, associated with the process Z:

$$N((0, t], B) := \#\{s \in (0, t] : \Delta Z_s \in B\}, \quad B \in \mathcal{B}(\mathbb{R} \setminus \{0\}),$$

and by $\widetilde{N}(dt, dz) := N(dt, dz) - dt\, \nu(dz)$ the compensated Poisson random measure. Here $\nu(\cdot)$ is the Lévy measure, associated with Z via the Lévy-Khinchin formula.

Throughout the paper we make the following standing assumptions:

- $\nu(\cdot)$ is absolutely continuous with respect to the Lebesgue measure;
- Z admits the Lévy-Ito decomposition:

$$Z_t = \int_0^t \int_{\mathbb{R}} z\widetilde{N}(ds, dz). \tag{1}$$

Consider a Lévy-driven SDE of the type

$$\begin{aligned} X_t = X_0 + \int_0^t a(s, X_s)\, ds + \int_0^t b(s, X_s)\, dB_s \\ + \int_0^t \int_{\mathbb{R}} c(s, X_{s-}, z)\widetilde{N}(ds, dz), \quad t > 0, \end{aligned} \tag{2}$$

where $a(s,x)$, $b(s,x)$, $c(s,x,z)$ are some deterministic measurable functions.

Protter and Talay [26] initiated the study of Euler schemes for such SDEs by analyzing errors for expectations of smooth test functions. Later, Jacod [10] extended this framework by proving limit theorems for Euler approximations and studying the asymptotic behavior of the normalized error process $u_n(X_t - X_t^n)$ for some appropriate scaling sequence $u_n \to \infty$. Of special interest are the SDEs driven by α-stable processes. For $\alpha \in [1, 2)$, strong convergence rates for the Euler–Maruyama approximation have been derived in [21, 22] and [17]; see also [20]. In parallel, Butkovsky et al. [5] investigated the strong convergence of the Euler–Maruyama scheme for multidimensional SDEs with β-Hölder drift ($\beta > 0$) driven by an α-stable Lévy process with $\alpha \in (0, 2]$. In particular, they established strong L^p-error bounds that are independent of p for $\alpha \in (2/3, 2]$ and demonstrated the optimality of these rates.

From a practical standpoint, simulation of such SDEs is challenging because the exact distribution of Lévy increments is generally unknown except for some special cases. Moreover, Lévy processes can exhibit countably many small jumps in any given finite interval, making direct simulation infeasible. Such a behavior is known as infinite activity:

$$\int_{\mathbb{R}} \nu(dz) = +\infty. \tag{3}$$

For processes with finite activity, simulation reduces to that of a compound Poisson process, but infinite activity requires alternative approaches. Asmussen and Rosiński [1] addressed this issue by replacing the cumulative effect of small jumps (those below a fixed threshold δ_{AR}) with a Gaussian term whose variance matches that of the truncated small jumps. In the one-dimensional multiplicative case $dX_t = \sigma(X_{t^-})\, dZ_t$, Fournier [7] analyzed the scheme with Gaussian replacement of jumps $|z| \le \delta_{\mathrm{AR}}$ and showed that choosing $\delta_{\mathrm{AR}} = n^{-1}$ yields mean-square error $O(n^{-1})$ at mean cost $O\big(n + \int_{|z|>1/n} \nu(dz)\big)$; in particular, if $\nu(\cdot)$ admits a density $g(z) \asymp |z|^{-1-\alpha}$ near 0, the cost scales as $O(n + n^{\alpha})$, whereas omitting the small jumps allows us to reach the same accuracy, requiring $\varepsilon = n^{-1/(2-\alpha)}$ and cost $O\big(n + n^{\alpha/(2-\alpha)}\big)$. Later, Bossy and Maurer [3] generalized that idea to the time-inhomogeneous jump-driven SDEs of type (2), and derived strong convergence rates for $p \geq 2$ together with an optimal choice of the fixed threshold.

While fixed-grid discretization schemes are straightforward to implement, they ignore the timing of jump events. To address this issue, Platen [24] and Bruti-Liberati and Platen [25] developed the class of jump-adapted strong Taylor schemes, where the simulation grid is explicitly synchronized with the jump times of the driving process. Although this construction eliminates the need to evaluate multiple stochastic integrals, it becomes computationally infeasible for infinite-activity Lévy processes due to the accumulation of small jumps. To resolve this bottleneck, Kohatsu-Higa and Tankov [15] proposed a hybrid thresholding approach: they retain a non-uniform grid based only on large jumps (exceeding a fixed threshold) and approximate the contribution of the small jumps between these points using a Brownian motion with matched variance.

The aim of this paper is to derive the strong convergence rates, relying on the *dynamic cutting* procedure, which we hope to be an accurate and effective tool for approximation of the process X. Dynamic cutting was introduced in [12, 11] for deriving the representation of transition probability density of a Lévy process and its small-time approximation, and developed later in [13, 14], where the transition probability of the solution to a Lévy-driven SDE or, more generally, some Lévy-type process, is constructed. The density in this case is written as a convolution of some "proxy" function and the kernel (which depends on this "proxy"). Such a representation is needed, for example, when one wants to get (upper or lower) estimates of functionals of type $\mathbb{E}^x f(X_t)$, where f is some (continuous) function. The transition probability density of a (time-inhomogeneous) process with the triplet $(0, 0, \mathbb{1}_{|u|\leq\phi(t)}\nu(y, du))$ plays the role of the "proxy", where $\mathbb{1}_{|u|\leq\phi(t)}\nu(y, du)$ is the Lévy measure, restricted to some time-dependent domain, which explains the name "dynamic cutting"; here y is some fixed point, and ϕ is the cutting level, depending on the measure ν. Although the analytical results from the above papers give a closed form of the transition probability density, it is technically hard to implement.

In this paper we want to elaborate a similar idea for simulations. Namely, we approximate the underlying Lévy process by a time-inhomogeneous compound Poisson process (which we abbreviate below as ICPP), obtained from Z by deleting small jumps together with their compensator in a time–dependent way. In contrast to [1],

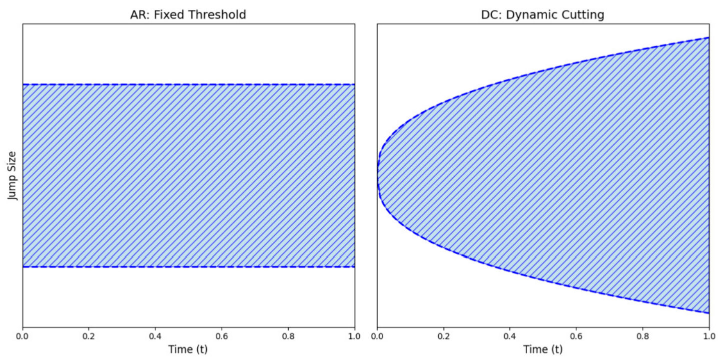

Fig. 1. AR vs DC

where the small jumps of fixed size were removed, we delete the jumps whose size depends on time (see Figure 1 and (5) for the definition of functions $\tau^{\pm}$). Such a construction is more flexible especially if implemented on a small-time interval.

Using the Euler scheme with the jump-adapted (or "adjusted") grid, we derive (cf. Theorem 3.1) the strong convergence rates in L^p for $p > \max\{\alpha, 1\}$, where α is a parameter, determined by the behavior of the Lévy measure $\nu(\cdot)$ near the origin.

We compare the dynamic cutting scheme with the classical Asmussen–Rosiński (AR) truncation under matched simulation cost (i.e., with the expected number of retained jumps made equal). On the test example the dynamic cutting (DC) approach demonstrates consistently smaller L^1–errors, which are still of the same order, when the jump coefficient has a time singularity near 0 (e.g., $|c(t,x,z)| \lesssim t^{-\sigma} g(x,z)$ with $\sigma > 0$). We have taken σ close to the critical values, because on them the difference between the methods is more distinct. If such a singularity is absent, DC (for given parameters) does not show a uniform advantage over AR. We also discuss the role of parameters ε and h used in the cutting function.

Dynamic cutting could be applied to models with singularities, for instance, to stochastic integrals of the form $\int_0^t K(t,s)dZ_s$, where the kernel is singular. In such a situation dynamic cutting allows a wider range of kernel singularities.

2 Settings

2.1 Preliminaries and assumptions

We write $f \lesssim g$ if there exists a generic constant $C > 0$ such that $f \le Cg$. The notation $f \asymp g$ means that $f \lesssim g$ and $g \lesssim f$. Since we are interested in the order of convergence, the particular constants are not crucial for us; therefore, we write $\lesssim$ or $\gtrsim$ instead of writing inequalities with explicit constants. For a Borel set A we write A^c for its complement. By $C_b^k(\mathbb{R})$ we denote the class of k-times differentiable functions with bounded derivatives. If not stated otherwise, we assume that $t \in [0,T]$, where $T > 0$ is the time horizon, and the parameter $\varepsilon \in (0,1)$, appearing in the cutting level, is fixed. We assume that the starting point $X_0 = x \in \mathbb{R}$ is non-random.

For $r > 0$ let

$$\begin{aligned} N^+(r) &:= \nu((r,\infty)), \quad N^-(r) := \nu((-\infty,-r)), \\ N(r) &:= N^+(r) + N^-(r). \end{aligned} \tag{4}$$

Denote the inverses of $N^{\pm}$ at t^{-1} for $t > 0$ by

$$\tau^{\pm}(t) := \sup\left\{ r \ge 0 : N^{\pm}(r) \ge \frac{1}{t} \right\}, \tag{5}$$

$$\tau(t) := \max\left(\tau^+(t), \tau^-(t)\right). \tag{6}$$

Denote by $\psi^{L,\pm}$, ψ^L the *lower Pruitt functions*, see [27]:

$$\psi^{L,\pm}(\xi) := \int_{|u\xi|\le 1} |u\xi|^2 \, \nu^{\pm}(du), \quad \psi^L(\xi) := \psi^{L,+}(\xi) + \psi^{L,-}(\xi), \tag{7}$$

where $\nu^+(du) = \nu(du)\mathbb{1}_{(0,\infty)}(u)$, $\nu^-(du) = \nu(du)\mathbb{1}_{(-\infty,0)}(u)$. Here the index L stands for the "lower"; together with the Pruitt's *upper function*, it plays an important role in existence and regularity of the transition probability density of Z_t, see Remark 4.1 in Section 4. Below we collect assumptions on $N^\pm(r)$ and coefficients $a(s,x)$, $b(s,x)$ and $c(s,x,z)$. In order to keep the presentation as transparent as possible, we postpone the detailed discussion of the conditions and their illustration to Section 4.

Assumption 1 (Kernel assumption)**.** Assume that the functions $\psi^{L,\pm}$ and $N^\pm$ are comparable:

$$\psi^{L,\pm}(1/r) \asymp N^\pm(r), \quad r \in (0,1].$$

Remark 2.1. It was shown in [9, Lem. 4.1] that Assumption 1 implies the doubling property of functions $N^\pm(r)$, i.e. $N^\pm(2r) \asymp N^\pm(r)$, which in turn implies the power decay of some order $\alpha^\pm \in (0,2)$ of $N^\pm(r)$ on $(0,1)$. Writing explicitly the constants in Assumption 1, one can find the parameters $\alpha^\pm$; see more details in Remark 4.1. This property ensures the bound on the inverse functions $\tau^\pm$:

$$\text{if} \qquad N^\pm(r) \le r^{-\alpha^\pm},\ r \in (0,1], \qquad \text{then} \qquad \tau^\pm(t) \lesssim t^{1/\alpha^\pm},\ t \in (0,1]. \tag{8}$$

Put

$$\alpha := \max\{\alpha^-, \alpha^+\} \tag{9}$$

and define the domain

$$B(s,h) := \left\{z \in \mathbb{R} : -\tau^-((sh)^\varepsilon) \le z \le \tau^+((sh)^\varepsilon)\right\}. \tag{10}$$

In what follows, we assume that the tuning parameter h belongs to some fixed interval, i.e. $h \in (0, h_0]$, where $h_0 \le 1$ fixed, and $\varepsilon \in (0,1)$.

Assumption 2 (Space and time regularity)**.** Assume that coefficients $a(s,x)$, $b(s,x)$, $c(s,x,z)$ are deterministic measurable functions, such that $a(t,0)$, $b(t,0)$ are bounded and satisfy the following conditions.

1. (Lipschitz condition) There exists a constant $L_{a,b} > 0$ and a measurable function $L_c : [0,T] \times \mathbb{R} \to \mathbb{R}_+$ such that for all $x, y, z \in \mathbb{R}$, $t \in (0,T]$,

$$|a(t,x) - a(t,y)| + |b(t,x) - b(t,y)| \le L_{a,b}|x-y|, \tag{11}$$

$$|c(t,x,z) - c(t,y,z)| \le L_c(t,z)|x-y|. \tag{12}$$

2. (Integrability) There exists $p > 1$ such that

$$\overline{L}_c(t,z) := \max\{L_c(t,z), |c(t,0,z)|\} \in L^p(\nu), \tag{13}$$

and

$$M_{p,h} \in L^\zeta([0,T]), \quad \zeta > 1, \tag{14}$$

uniformly in $h \in (0, h_0]$, where

$$M_{p,h}(t) := \begin{cases} \displaystyle\int_{B^c(t,h)} |\overline{L}_c(t,z)|^p\, \nu(dz), & 1 < p < 2, \\ \displaystyle\int_{B^c(t,h)} |\overline{L}_c(t,z)|^p\, \nu(dz) & \\ \qquad + \left(\displaystyle\int_{B^c(t,h)} |\overline{L}_c(t,z)|^2\, \nu(dz)\right)^{p/2}, & p \ge 2. \end{cases} \tag{15}$$

3. (Peano condition) There exists a real number $\gamma \in (0,1]$ such that for all $x, y \in \mathbb{R}$, $s, t \in [0,T]$
$$|a(t,x) - a(s,x)| + |b(t,x) - b(s,x)| \leq L_{a,b}|t-s|^\gamma(1+|x|). \tag{16}$$
4. (Boundedness) There exists $\sigma \geq 0$ such that for all $x \in \mathbb{R}$, $t \in (0,T]$, $z \in B(t,h)$ we have
$$L_c(t,z) \lesssim t^{-\sigma}|z|, \tag{17}$$
$$|c(t,x,z)| \lesssim t^{-\sigma}(1+|x|)|z|. \tag{18}$$
5. (Large-jump compensator) Assume that either the retained compensator is centered,
$$\int_{B^c(t,h)} c(t,x,z)\nu(dz) = 0, \tag{19}$$
for all $x \in \mathbb{R}$, $t \in (0,T]$, $h \in (0,h_0]$, or
$$M_{1,h}(t) := \int_{B^c(t,h)} \overline{L}_c(t,z)\nu(dz) \lesssim t^{-\chi}, \quad \chi \in (0,1), \tag{20}$$
uniformly in $h \in (0,h_0]$.

Remark 2.2. Condition (19) is clearly satisfied provided that the measure ν is symmetric and $c(t,x,z)$ is anti-symmetric for all x and t. The important part about condition (20) is the uniform boundedness in h, which does not immediately follow from (14) because $\nu(B^c(t,h))$ is unbounded in h near 0. For example, let $c(t,x,z) = \sin(x)(1 \wedge |z|)$ and let $\nu(\cdot)$ be a symmetric alpha-stable Lévy measure with $\alpha \in (0,1)$. Since $c(t,0,z) = 0$ and
$$|c(t,x,z) - c(t,y,z)| \leq (1 \wedge |z|)|x-y|,$$
we may take $\overline{L}_c(t,z) = L_c(t,z) = 1 \wedge |z|$. Hence, uniformly in h,
$$M_{1,h}(t) \leq \int_{\mathbb{R}} (1 \wedge |z|)\nu(dz) \asymp \int_0^1 r^{-\alpha}\,dr + \int_1^\infty r^{-1-\alpha}\,dr < \infty.$$
Thus, on $(0,T]$, $M_{1,h}(t) \lesssim t^{-\chi}$ for any $\chi \in (0,1)$, and (20) holds.

Remark 2.3. The spatial Lipschitz and temporal integrability conditions in Assumptions 2 and 2.2 guarantee the existence of the unique strong solution to (2) adapted to $(\mathcal{F}_t)_{t\geq 0}$. For $p = 2$ we refer to [8, Th.IV.9.1]. This argument extends, however, for $p > 1$, using Kunita-type maximal inequalities. More precisely, one combines Kunita's Burkholder-Davis-Gundy inequality (later: BDG) with the Cauchy-Schwarz inequality (for $p \geq 2$), while for $p \in (1,2)$ one uses Novikov's version of BDG together with Young's inequality to construct the required inequalities. This yields the standard bounds on $\mathbb{E}\sup_{s\leq t}|X_s|^p$; the existence, uniqueness and L^p estimates follow from the Gronwall inequality and Picard iterations. For the complete proof in the case $p \geq 2$ see [4]. Similar technical trick in the case $p \in (1,2)$ and zero diffusion coefficient was used in Lemma A.7 in Appendix. Alternatively, one can rely on [16, Th.4.1].

2.2 Euler scheme

The Euler scheme used in the paper involves an adjusted grid, which is constructed by adding to the given uniform grid the jump times of a compound Poisson process. Below we explain this construction.

Let $\pi_n := \{0 = t_0 < s_1 < \cdots < s_{n-1} < s_n = T\}$ be a uniform partition of the interval $[0, T]$, i.e. $s_i = s_{i-1} + \Delta$, $\Delta = T/n$, $1 \le i \le n$. Define

$$Z_h^{CP,+}(t) := \sum_{s \le t} \Delta Z_s \mathbb{1}_{\Delta Z_s \ge \tau^+((sh)^\varepsilon)}, \quad Z_h^{CP,-}(t) := \sum_{s \le t} \Delta Z_s \mathbb{1}_{\Delta Z_s \le -\tau^-((sh)^\varepsilon)}. \quad (21)$$

These processes are obtained by dynamic cutting away the jumps of the underlying Lévy process Z at the levels $\tau^+((sh)^\varepsilon)$ and $-\tau^-((sh)^\varepsilon)$, respectively.

It can be shown (cf. Section 6.1), that $Z_h^{CP,\pm}$ are ICPPs; moreover, their intensities are equal to

$$N^\pm(\tau^\pm((th)^\varepsilon)) = (th)^{-\varepsilon}.$$

The assumption that $\varepsilon \in (0, 1)$ is essential and guarantees that the integral intensity

$$\lambda_h(t) := \frac{t^{1-\varepsilon}}{1-\varepsilon} h^{-\varepsilon}$$

is finite. Both parameters h and ε are responsible for the average numbers of jumps of $Z_h^{CP,\pm}$ on the time interval $[0, t]$, which are equal to $\lambda_h(t)$.

Define by $T_i^\pm$, $i \ge 1$, the jump times of $Z_h^{CP,\pm}(t)$, respectively. We add to the partition π_n the sets of points $S^\pm := \{T_i^\pm : T_i^\pm \le T\}_{i \ge 1}$, see Figure 2 below for the adjusted grid

$$\Pi := \pi_n \cup S^+ \cup S^-. \quad (22)$$

Note that the elements t_i of the grid Π are $\mathcal{F}_{t_i}$ – measurable. Denote by $\sharp jumps[0, t]$ the total number of jumps of $Z_h^{CP,+} + Z_h^{CP,-}$ on $[0, t]$, and by $\rho(t) = \sharp jumps[0, t] + [tn/T]$ the total number of points in the adjusted grid on $[0, t]$; here $[x]$ denotes the integer part of $x \in \mathbb{R}$. From above, $\rho(t)$ is random and for fixed t

$$\mathbb{E}\rho(t) = \left[\frac{tn}{T}\right] + 2\lambda_h(t). \quad (23)$$

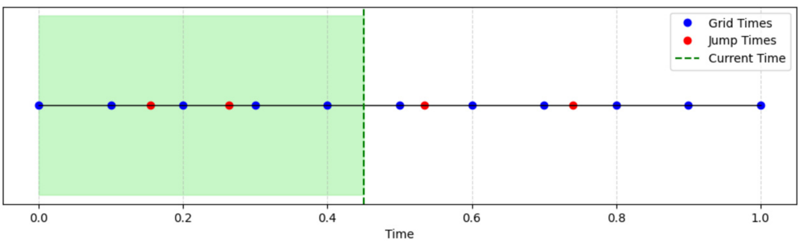

Fig. 2. Grid and Jump Times

For $i = 1, \ldots, \rho(T)$, let $\Delta_i := (t_i - t_{i-1})$, $\Delta B_i := B_{t_i} - B_{t_{i-1}}$,

$$\widetilde{a}(t_{i-1}, t_i, x) := a(t_{i-1}, x) - \Delta_i^{-1} \int_{t_{i-1}}^{t_i} \int_{B^c(s,h)} c(s, x, z) \nu(dz)\, ds. \quad (24)$$

Set $X_0^\tau = x$, and define

$$X_{t_i}^\tau := X_{t_{i-1}}^\tau + \widetilde{a}(t_{i-1}, t_i, X_{t_{i-1}}^\tau)\Delta_i + b(t_{i-1}, X_{t_{i-1}}^\tau)\Delta B_i + C_i(X_{t_{i-1}}^\tau), \tag{25}$$

where

$$C_i(x) := c(t_i, x, \Delta Z_{t_i})\mathbb{1}_{\{t_i \in S^+\}} + c(t_i, x, \Delta Z_{t_i})\mathbb{1}_{\{t_i \in S^-\}}$$

is the large-jump increment occurring at time $t_i \in \Pi$.

We also put $X_t^\tau = X_{t_i}^\tau$ for $t \in [t_i, t_{i+1})$.

Notation

For the convenience of the reader, we collect the essential notation used throughout the paper in Table 1.

Table 1. Key notation and definitions

Symbol	Meaning
ε, h	Dynamic cutting parameters
σ	Time-singularity exponent for $c(t, x, z)$ near $t = 0$ (see (18)).
γ	Hölder index of time regularity of $a(t, x)$ and $b(t, x)$
$\tau^\pm(t)$, $\tau(t)$	Generalized inverse functions (see (5)), $\tau(t) = \max\{\tau^+(t), \tau^-(t)\}$.
$B(s, h)$	Small-jump region removed by cutting (see (10)).
$B^c(s, h)$	Complement (large-jump region).
π_n	Uniform grid on $[0, T]$ with $\Delta = T/n$.
$Z_h^{CP,\pm}(t)$	Large-jump inhomogeneous compound Poisson process.
$S^\pm$, Π	Jump times of $Z_h^{CP,\pm}$ on $[0, T]$, $\Pi = \pi_n \cup S^+ \cup S^-$.
$\rho(t)$	Number of points of Π up to time t.
$\eta(t)$	Previous grid time: $\eta(t) = \sup\{s \in \Pi : s \le t\}$.
$\widetilde{X}_t$	Peano scheme with frozen coefficients (see (34)).
X_t^τ	Euler scheme on Π with dynamic cutting (see (25)).
θ_*	(26)
β	$\beta = \min(\gamma, 1/2, 1 - \chi)$
κ	$\kappa = \min(1, 2(1 - \theta_*))$

3 Main results

Recall the definition of α, cf. (9). Let

$$\theta_* := \begin{cases} p\sigma - \frac{\varepsilon(p-\alpha)}{\alpha}, & p < 2, \\ p\sigma - \frac{\varepsilon p(2-\alpha)}{2\alpha}, & p \ge 2. \end{cases} \tag{26}$$

Further, let $\beta := \min(\gamma, 1/2, 1 - \chi)$, $\kappa := \min\{1, 2(1 - \theta_*)\}$, and

$$\mathcal{R}_p(n, h) := \begin{cases} n^{-\beta} + n^{-\frac{\kappa}{p}} h^{\frac{2(\sigma p - \theta_*)}{p}} (1 + \mathbb{1}_{\{\theta_* = \frac{1}{2}\}} \ln n), & p < 2, \\ n^{-\beta} + n^{-\frac{1}{p}} h^{\frac{\sigma p - \theta_*}{p}} + n^{-\frac{\kappa}{p}} h^{\frac{2(\sigma p - \theta_*)}{p}} (1 + \mathbb{1}_{\{\theta_* = \frac{1}{2}\}} \ln n), & p \ge 2. \end{cases} \tag{27}$$

If (19) is satisfied, we put $\chi = 0$.

Theorem 3.1. *Suppose that Assumptions 1 – 2 are satisfied. Let p and ζ be the parameters appearing in* (13) – (15)*, and $\sigma \geq 0$ be the parameter from* (18)*. Suppose that $\theta_* < \frac{\zeta-1}{\zeta}$ and either a) or b) hold true:*

a) $p \geq 2$;

b) $p \in (\max\{1, \alpha\}, 2)$ *and* $b(t, x) \equiv 0$.

Then,

1.

$$\Big\| \sup_{t_i \in \Pi} |X_{t_i} - X^\tau_{t_i}| \Big\|_{L^p(\Omega)} \lesssim \mathcal{R}_p(n, h) + h^{\frac{\sigma p - \theta_*}{p}}. \tag{28}$$

2.

$$\sup_{t \in [0,T]} \Big\| X_t - X^\tau_t \Big\|_{L^p(\Omega)} \lesssim \mathcal{R}_p(n, h) + h^{\frac{\sigma p - \theta_*}{p}}. \tag{29}$$

Remark 3.1. The right-hand sides of (28) and (29) contain the Euler–Peano discretization contribution $\mathcal{R}_p(n, h)$ and the dynamic-cutting truncation contribution $h^{(\sigma p - \theta_*)/p}$. Under the balancing choice

$$h = h(n) \asymp \begin{cases} n^{-\frac{\beta p \alpha}{\varepsilon(p-\alpha)}}, & p < 2, \\ n^{-\frac{2\beta\alpha}{\varepsilon(2-\alpha)}}, & p \geq 2. \end{cases} \tag{30}$$

one gets (up to the logarithmic factor present in $\mathcal{R}_p(n, h)$ when $\theta_* = \frac{1}{2}$)

$$\sup_{t \in [0,T]} \|X_t - X^\tau_t\|_{L^p(\Omega)} \lesssim n^{-\beta}.$$

Remark 3.2 (Dependence on p)**.**

a) The bound (28) contains two terms with opposite p-dependence: $\mathcal{R}_p(n, h)$ and $h^{(\sigma p - \theta_*)/p}$. From the definition of θ_*,

$$h^{(\sigma p - \theta_*)/p} = \begin{cases} h^{\varepsilon(p-\alpha)/(\alpha p)}, & p < 2, \\ h^{\varepsilon(2-\alpha)/(2\alpha)}, & p \geq 2. \end{cases}$$

For $p < 2$, the exponent of h is strictly increasing in p (the cutting error improves as $p \to 2$), whereas for $p \geq 2$ it is constant. In contrast, $\mathcal{R}_p(n, h)$ contains factors such as $n^{-1/p}$ and $n^{-\kappa/p}$, which improve as p decreases. So the bound is not monotone: for $p < 2$ there is a trade-off between the terms, while for $p \geq 2$, decreasing p strictly improves the discretization/cutting part of the bound.

b) The first term on the right-hand side of (28) is responsible for the discretization error, arising from switching from X_t to the Peano scheme $\widetilde{X}_t$ (cf. (34) below), which is uniform in t, whereas the second term is responsible for the error arising from discarding small jumps. In (29), we add the error arising from switching from $\widetilde{X}_{t_i}$ to $\widetilde{X}_t$. This error contains the same contributions from the right-hand side of (28).

Remark 3.3. Theorem 3.1 allows a generalization to a multi-dimensional setting. Assumption 1 (as it is formulated) is purely one-dimensional and reflects the fact that the cutting level for each tail of the Lévy measure might be different. Unless we assume that there exists a density of the Lévy measure on $\mathbb{R}^d$, and it is comparable with a radially symmetric function, such a generalization is not straightforward.

4 Discussion and examples

We provide simple examples, where Assumptions 1 and 2 are satisfied.

Example 4.1. Let

$$\nu(du) = \frac{|\ln|u||^\rho}{|u|^{1+\alpha}} \mathbb{1}_{0<|u|<1}\, du, \qquad \alpha \in (0,2),\ \rho > -1.$$

For $0 < r < 1$,

$$\psi^{L,+}(1/r) = \int_0^r |u/r|^2 \nu^+(du) = r^{-2} \int_0^r u^{1-\alpha} |\ln u|^\rho\, du.$$

The function $L(u) := |\ln u|^\rho$, $u > 0$, is slowly varying at 0. Then substituting $u = 1/t$ and applying Karamata's theorem (see [2, Prop.1.5.8]), we obtain

$$\int_0^r u^{1-\alpha} L(u)\, du \sim \frac{r^{2-\alpha}}{2-\alpha} L(r), \quad r \to 0,$$

hence

$$\psi^{L,+}(1/r) \sim \frac{1}{2-\alpha} r^{-\alpha} |\ln r|^\rho, \quad r \to 0. \tag{31}$$

On the other hand, by [2, Prop.1.5.10],

$$N^+(r) = \int_r^1 \frac{|\ln u|^\rho}{u^{1+\alpha}}\, du \sim \frac{1}{\alpha} r^{-\alpha} |\ln r|^\rho, \quad r \to 0. \tag{32}$$

Therefore

$$\frac{\psi^{L,+}(1/r)}{N^+(r)} \longrightarrow \frac{\alpha}{2-\alpha} \in (0,\infty),$$

so $\psi^{L,+}(1/r) \asymp N^+(r)$, which verifies Assumption 1 for $\psi^{L,+}$ and N^+. By symmetry of the Lévy measure, Assumption 1 is satisfied also for the pair $\psi^{L,-}$ and N^-.

Note that the same result holds true for the measure

$$\nu(du) = \frac{|\ln|u||^\rho}{|u|^{1+\alpha}}\, du, \qquad u \in \mathbb{R},\ \alpha \in (0,2),\ \rho > -1.$$

Indeed, the argument for $\psi^{L,+}$ remains the same, and the asymptotic behavior of $N(r)$ at 0 in the case of non-cut measure is clearly the same as that of the cut one. The restriction $\rho > -1$ is caused by the singularity of $|\ln|u||^\rho$ for $\rho \le -1$ and can be removed by replacing $\ln|u|$ with $\ln(1+|u|)$. In this case the asymptotic behavior (31) and (32) remains valid for all $\rho \in \mathbb{R}$.

Next, for simplicity assume that $a(t,x) = b(t,x) = 0$, and for $\sigma \in [0,1)$ define

$$c(t,x,z) := t^{-\sigma}\ \tanh(x)\ \min\{|z|,1\}, \qquad t \in (0,T],\ x,z \in \mathbb{R}.$$

Then $c(t,0,z) = 0$ and $\partial_x c(t,x,z) = t^{-\sigma}\ \min\{|z|,1\}\ \mathrm{sech}^2(x)$. Thus,

$$\left|\partial_x c(t,x,z)\right| \le t^{-\sigma}\ \min\{|z|,1\} =: L_c(t,z),$$

so that condition (12) is clearly satisfied. Assumption 2.4 is clearly satisfied, since $|\tanh(x)| \le 1$. Let us check the integrability assumptions (13) and (14) for $c(t,x,z)$ and the α-stable Lévy measure. If $p > \alpha$, it is easy to see that $\int_{\mathbb{R}} \min\{1, |z|^p\}\nu(dz) < \infty$, and $\int_{B^c(t,h)} L_c^p(t,z)\nu(dz) \lesssim t^{-\sigma p}$, $t \in (0,T]$, uniformly in h. Hence, (14) is satisfied whenever $\zeta\sigma p < 1$. Finally, (20) is satisfied when $\alpha < 1$ and $\sigma < 1$. Thus, for $c(t,x,z)$ and ν as above all conditions of Assumption 2 are satisfied, if $\alpha \in (0,1)$. If we modify $c(t,x,z)$ in such a way that it is anti-symmetric in z, then Assumption 2 is satisfied for all $\alpha \in (0,2)$.

Example 4.2. One can substitute the α-stable Lévy measure in Example 4.1 with the truncated one: $\nu(dz) = \mathbb{1}_{\{|z|<1\}}\,|z|^{-(1+\alpha)}dz$, $\alpha \in (0,2)$. Straightforward calculation shows that Assumption 1 is satisfied. Indeed, for $r \in (0,1)$ we have

$$N^-(r) = N^+(r) = \int_r^1 |z|^{-(1+\alpha)}\, dz = \frac{r^{-\alpha}-1}{\alpha}. \tag{33}$$

By (7), $\psi^{L,+}\left(\frac{1}{r}\right) = \frac{r^{-\alpha}}{2-\alpha}$, $\psi^{L,-} = \psi^{L,+}$. Thus, $\psi^{L,\pm}(1/r) \asymp N^{\pm}(r)$ on $(0,1]$.

Remark 4.1 (On Pruitt functions)**.** Assume for simplicity that the Lévy measure is symmetric. Pruitt functions $\psi^L(\xi)$ and $\psi^U(\xi) := \psi^L(\xi) + N(|\xi|^{-1})$ are used to control regularity of the distribution of a Lévy process with Lévy triple $(0,0,\nu)$. The lower Pruitt function ψ^L does not need to be monotone, whereas $N(r)$ is monotonically decaying on $(0,\infty)$. Assumption 1 means that we can control oscillations of ψ^L. Note that for a Lévy process with Lévy triple $(0,0,\nu)$ with symmetric ν, the function $\psi(\xi) = \int_{\mathbb{R}}(1-\cos(\xi u))\nu(du)$ is the characteristic exponent of X_1 (i.e., the negated logarithm of the characteristic function), and

$$(1-\cos 1)\psi^L(\xi) \le \psi(\xi) \le 2(\psi^L(\xi) + N(|\xi|^{-1})).$$

Consequently, the control on the lower Pruitt function implies the control (for large $|\xi|$) on the characteristic exponent of the respective Lévy process, and thereby determines the behavior of the transition probability density of the Lévy process. See [12] for more about a condition similar to Assumption 1 and examples, where it is satisfied. Here we only mention, that if for $\mathfrak{w} \ge 1$ we have $\psi^U(\xi) \le \mathfrak{w}\psi^L(\xi)$, $|\xi| \ge 1$, then $\psi^L(\xi) \gtrsim |\xi|^{2/\mathfrak{w}}$, $|\xi| \ge 1$, in particular, Assumption 1 implies the power growth of $\psi^L(\xi)$ and $N(1/|\xi|)$ as $|\xi| \to \infty$.

5 Proof of Theorem 3.1

Let $\eta(t) := \sup\{t_n : t_n \le t\}$, where $t_i \in \Pi$, and recall that $\rho(t) = \sharp\{k : t_k \le t,\ t_k \in \Pi\}$. Note that $\eta(t) = t_{i-1}$ for each $t \in [t_{i-1}, t_i)$, $1 \le i \le \rho(T)$, and by definition

$\eta(t), \rho(t)$ are $\mathcal{F}_t$ – measurable. Write the Peano scheme with frozen coefficients for (2):

$$\widetilde{X}_t = x + \int_0^t a(\eta(s), \widetilde{X}_{\eta(s)})\, ds + \int_0^t b(\eta(s), \widetilde{X}_{\eta(s)})\, dB_s \\ + \int_0^t \int_{-\infty}^{+\infty} c(s, \widetilde{X}_{\eta(s-)}, z)\, \widetilde{N}(ds, dz). \tag{34}$$

Applying Remark 2.3 to the process $\widetilde{X}$, which is a solution to an SDE with piece-wise constant coefficients, one can see that $\widetilde{X}$ possesses p – moments for p as in the assumptions of Theorem 3.1.

We distinguish two cases $p < 2$ and $p \geq 2$, having in mind that p belongs to the intervals, defined in Theorem 3.1.

One can also rewrite (25) using the step function $\eta(t)$:

$$X^\tau_{\eta(t)} = X^\tau_0 + \int_0^{\eta(t)} a(\eta(s), X^\tau_{\eta(s)})\, ds + \int_0^{\eta(t)} b(\eta(s), X^\tau_{\eta(s)})\, dB_s \\ + \int_0^{\eta(t)} \int_{B^c(s,h)} c(s, X^\tau_{\eta(s-)}, z) \widetilde{N}(ds, dz). \tag{35}$$

Split

$$\left\| \sup_{s\leq t} \left| X_{\eta(s)} - X^\tau_{\eta(s)} \right| \right\|_{L^p(\Omega)} \\ \leq \left\| \sup_{s\leq t} \left| X_{\eta(s)} - \widetilde{X}_{\eta(s)} \right| \right\|_{L^p(\Omega)} + \left\| \sup_{s\leq t} \left| \widetilde{X}_{\eta(s)} - X^\tau_{\eta(s)} \right| \right\|_{L^p(\Omega)}. \tag{36}$$

The estimate for the first term is provided in Lemma A.7 in the Appendix. Note that for the case $p \geq 2$, this statement is proved in [3, Lem.3.1] for the uniform grid. In order to make our presentation self-contained, we provide the complete proof for all ranges p from statements a),b) of Theorem 3.1 and the adjusted grid in Lemma A.7 in the Appendix.

Now we estimate the norm $\Phi_h(t) := \left\| \sup_{s\leq t} \left| \widetilde{X}_{\eta(s)} - X^\tau_{\eta(s)} \right| \right\|_{L^p(\Omega)}$.

By the definition of $\eta(t)$, the difference between $\widetilde{X}_{t_i}$ and $X^\tau_{t_i}$ equals

$$\begin{aligned} \widetilde{X}_{\eta(t)} - X^\tau_{\eta(t)} = &\int_0^{\eta(t)} \Big(a(\eta(s), \widetilde{X}_{\eta(s)}) - a(\eta(s), X^\tau_{\eta(s)}) \Big)\, ds \\ &+ \int_0^{\eta(t)} \Big(b(\eta(s), \widetilde{X}_{\eta(s)}) - b(\eta(s), X^\tau_{\eta(s)}) \Big)\, dB_s \\ &+ \int_0^{\eta(t)} \int_{B^c(s,h)} \Big(c(s, \widetilde{X}_{\eta(s-)}, z) - c(s, X^\tau_{\eta(s-)}, z) \Big)\, \widetilde{N}(ds, dz) \\ &+ \int_0^{\eta(t)} \int_{B(s,h)} c(s, \widetilde{X}_{\eta(s-)}, z) \widetilde{N}(ds, dz). \end{aligned}$$

Applying Minkowski's inequality we can decompose the L^p-norm for $p > 1$ into the sum of four terms,

$$\left\|\widetilde{X}_{\eta(t)} - X^{\tau}_{\eta(t)}\right\|_{L^p(\Omega)} \leq \underbrace{(\text{drift})}_{\textbf{(A)}} + \underbrace{(\text{diffusion})}_{\textbf{(B)}} + \underbrace{(\text{large jumps})}_{\textbf{(C)}} + \underbrace{(\text{small jumps})}_{\textbf{(D)}}, \quad (37)$$

which we estimate separately.

Estimation of (A). Applying subsequently Minkowski's integral inequality and the Lipschitz assumption (11), we derive

$$\begin{aligned}
\textbf{(A)} &:= \left\|\int_0^{\eta(t)} \left(a(\eta(s), \widetilde{X}_{\eta(s)}) - a(\eta(s), X^{\tau}_{\eta(s)})\right) \mathbb{1}_{s\leq\eta(t)} ds\right\|_{L^p(\Omega)} \\
&\leq \int_0^t \left\|a(\eta(s), \widetilde{X}_{\eta(s)}) - a(\eta(s), X^{\tau}_{\eta(s)})\right\|_{L^p(\Omega)} ds \\
&\leq L_{a,b} \int_0^t \left\|\widetilde{X}_{\eta(s)} - X^{\tau}_{\eta(s)}\right\|_{L^p(\Omega)} ds \\
&\lesssim \int_0^t \Phi_h(s) ds.
\end{aligned}$$

Note that in this calculation the $\mathcal{F}_t$ – measurability of $\eta(t)$ is enough, but since $\eta(t)$ is not a stopping time, we cannot apply the same trick with the indicator to the other terms; instead, a different argument is required.

Estimation of (B). *Case 1: $p \geq 2$.* For the second term, we use that $\eta(t) \leq t$, the Burkholder-Davis-Gundy (BDG) inequality for continuous martingales, and again the Lipschitz assumption (11):

$$\begin{aligned}
\textbf{(B)} &:= \left\|\int_0^{\eta(t)} \left(b(\eta(s), \widetilde{X}_{\eta(s)}) - b(\eta(s), X^{\tau}_{\eta(s)})\right) dB_s\right\|_{L^p(\Omega)} \\
&\leq \left\|\sup_{r\in[0,t]} \left|\int_0^r \left(b(\eta(s), \widetilde{X}_{\eta(s)}) - b(\eta(s), X^{\tau}_{\eta(s)})\right) dB_s\right|\right\|_{L^p(\Omega)} \\
&\leq \left(C_p^{BDG}\right)^{\frac{1}{p}} \left(\int_0^t \left\|b(\eta(s), \widetilde{X}_{\eta(s)}) - b(\eta(s), X^{\tau}_{\eta(s)})\right\|^2_{L^p(\Omega)} ds\right)^{\frac{1}{2}} \\
&\leq \left(C_p^{BDG}\right)^{\frac{1}{p}} L_{a,b} \left(\int_0^t \left\|\widetilde{X}_{\eta(s)} - X^{\tau}_{\eta(s)}\right\|^2_{L^p(\Omega)} ds\right)^{\frac{1}{2}} \\
&\lesssim \left(\int_0^t \Phi_h^2(s)\, ds\right)^{\frac{1}{2}}.
\end{aligned}$$

If $p < 2$, then condition b) of Theorem 3.1 gives $b \equiv 0$, and hence $\textbf{(B)} = 0$.

Estimation of (C). To shorten the notation, denote

$$F(s, z) := \left(c(s, \widetilde{X}_{\eta(s-)}, z) - c(s, X^{\tau}_{\eta(s-)}, z)\right).$$

We handle the term with the large jumps using the maximal inequalities for martingales with jumps.

Case 1. $p \geq 2$. Applying Kunita's inequality (cf. [18, Th.4.20]), we get

$$\begin{aligned}
\textbf{(C)} &:= \left\| \int_0^{\eta(t)} \int_{B^c(s,h)} \left(c(s, \widetilde{X}_{\eta(s-)}, z) - c(s, X^{\tau}_{\eta(s-)}, z) \right) \widetilde{N}(ds, dz) \right\|_{L^p(\Omega)} \\
&\leq \left(\mathbb{E} \sup_{r \in [0,t]} \left| \int_0^r \int_{B^c(s,h)} F(s,z) \widetilde{N}(ds, dz) \right|^p \right)^{\frac{1}{p}} \\
&\lesssim \left(\mathbb{E} \left(\int_0^t \int_{B^c(s,h)} |F(s,z)|^2 \, \nu(dz) ds \right)^{p/2} \right)^{\frac{1}{p}} \\
&\quad + \left(\mathbb{E} \int_0^t \int_{B^c(s,h)} |F(s,z)|^p \, \nu(dz) \, ds \right)^{\frac{1}{p}}.
\end{aligned}$$

Case 2: $p < 2$. We apply Novikov's inequality with $a = p$ (cf. [18, Th.4.20]):

$$\begin{aligned}
\textbf{(C)} &:= \left\| \int_0^{\eta(t)} \int_{B^c(s,h)} F(s,z) \, \widetilde{N}(ds, dz) \right\|_{L^p(\Omega)} \\
&\leq \left\| \sup_{r \in [0,t]} \left| \int_0^r \int_{B^c(s,h)} F(s,z) \, \widetilde{N}(ds, dz) \right| \right\|_{L^p(\Omega)} \\
&\lesssim \left(\mathbb{E} \int_0^t \int_{B^c(s,h)} \left| F(s,z) \right|^p \nu(dz) \, ds \right)^{1/p}.
\end{aligned}$$

Using the Lipschitz assumption (12) and combining both cases, we obtain

$$\textbf{(C)} \lesssim \left(\int_0^t \Phi_h^p(s) M_{p,h}(s) \, ds \right)^{\frac{1}{p}}.$$

Estimation of (D). Let us estimate

$$I_h := \left\| \int_0^{\eta(t)} \int_{B(s,h)} c(s, \widetilde{X}_{\eta(s-)}, z) \, \widetilde{N}(ds, dz) \right\|_{L^p(\Omega)}.$$

In this part of the proof we use the upper estimate (18) from Assumption 2.

Case 1: $p \geq 2$. Applying Kunita's BDG inequality (cf. [18, Th.4.20]), we get

$$\begin{aligned}
I_h^p &\lesssim \int_0^t \mathbb{E} \left(\int_{B(s,h)} |c(s, \widetilde{X}_{\eta(s)}, z)|^2 \nu(dz) \right)^{p/2} ds \\
&\quad + \mathbb{E} \int_0^t \int_{B(s,h)} |c(s, \widetilde{X}_{\eta(s)}, z)|^p \nu(dz) \, ds.
\end{aligned}$$

According to Lemma A.3 and (8),

$$\int_0^t \mathbb{E}\left(\int_{B(s,h)} |c(s, \widetilde{X}_{\eta(s)}, z)|^2 \nu(dz)\right)^{p/2} ds \lesssim \int_0^t \frac{(\tau((sh)^\varepsilon))^p s^{-\sigma p}}{(sh)^{\varepsilon p/2}} ds$$
$$\lesssim h^{\frac{\varepsilon p(2-\alpha)}{2\alpha}} \int_0^T s^{-\sigma p + \frac{\varepsilon p(2-\alpha)}{2\alpha}} ds$$
$$\lesssim h^{\frac{\varepsilon p(2-\alpha)}{2\alpha}}.$$

Note that the condition $p\sigma < 1 + \frac{\varepsilon p(2-\alpha)}{2\alpha}$ implies that $p\sigma + \varepsilon < 1 + \frac{\varepsilon p}{\alpha}$. Then, applying Lemma A.6.ii), we derive that the second term is bounded by

$$\mathbb{E} \int_0^t \int_{B(s,h)} |c(s, \widetilde{X}_{\eta(s)}, z)|^p \nu(dz)\, ds \lesssim h^{\frac{\varepsilon(p-\alpha)}{\alpha}}.$$

Since $0 < h < 1$, then $h^{-\varepsilon p/2} > h^{-\varepsilon}$. Therefore,

$$I_h^p \lesssim h^{\frac{\varepsilon p(2-\alpha)}{2\alpha}}.$$

Case 2: $p < 2$. We apply Novikov's BDG inequality and Lemma A.5 combined with the bound $\tau(t) \lesssim t^{1/\alpha}$ from (8). We observe that the assumption $\theta_* < 1$, $\theta_* = p\sigma - \frac{\varepsilon(p-\alpha)}{\alpha}$ for $p < 2$, ensures that the integral converges. In addition, we use the moment bound $\sup_{s\le T} \mathbb{E}(1 + |\widetilde{X}_s|^p) < \infty$. Thus,

$$I_h^p \lesssim \mathbb{E} \int_0^t s^{-p\sigma} \tau^{p-\alpha}((sh)^\varepsilon)\, ds \lesssim h^{\frac{\varepsilon(p-\alpha)}{\alpha}} \int_0^t s^{-p\sigma + \frac{\varepsilon(p-\alpha)}{\alpha}} ds \lesssim h^{\frac{\varepsilon(p-\alpha)}{\alpha}}.$$

Consequently,

$$I_h \lesssim h^{\frac{\varepsilon(p-\alpha)}{p\alpha}}.$$

Completing the proof. We combine the bounds for terms (A)–(D), and arrive at

$$\Phi_h(t) \lesssim \int_0^t \Phi_h(s)\, ds + \mathbb{1}_{\{p\ge 2\}} \left(\int_0^t \Phi_h^2(s)\, ds\right)^{1/2}$$
$$+ \left(\int_0^t \Phi_h^p(s) M_{p,h}(s)\, ds\right)^{1/p} + r(h), \tag{38}$$

where

$$r(h) = \begin{cases} h^{\frac{\varepsilon(p-\alpha)}{p\alpha}}, & p < 2, \\ h^{\frac{\varepsilon(2-\alpha)}{2\alpha}}, & p \ge 2. \end{cases}$$

Using Gronwall's inequality (see Theorem B.1), we get

$$\Phi_h(t) \lesssim e^{Ct} r(h) \implies \sup_{0\le t\le T} \Phi_h(t) \lesssim r(h). \tag{39}$$

Adding the error from the Euler–Peano approximation we derive the upper bounds in cases a) and b) for $\left\|\sup_{s\le T} |X_{\eta(s)} - X^\tau_{\eta(s)}|\right\|_{L^p(\Omega)}$. Combining with Lemma A.7, we get (28).

To show (29), observe that

$$\|X_t - X_t^\tau\|_{L^p(\Omega)} \le \left\|X_t - \widetilde{X}_t\right\|_{L^p(\Omega)} + \left\|\widetilde{X}_t - \widetilde{X}_{\eta(t)}\right\|_{L^p(\Omega)} + \left\|\widetilde{X}_{\eta(t)} - X^\tau_{\eta(t)}\right\|_{L^p(\Omega)}. \tag{40}$$

Estimate for the first term is proved in Lemma A.7. For the second term, put $\Delta := T/n$. If $\theta_* \ge 0$, then applying (61) yields

$$\left\|\widetilde{X}_t - \widetilde{X}_{\eta(t)}\right\|_{L^p(\Omega)} \lesssim n^{-\beta} + n^{-\frac{1-\theta_*}{p}} h^{\frac{\sigma p-\theta_*}{p}}, \tag{41}$$

uniformly in $t \in [0, T]$. If $\theta_* < 0$, then $s^{-\theta_*/p} \le T^{-\theta_*/p}$, and (61) yields instead

$$\left\|\widetilde{X}_t - \widetilde{X}_{\eta(t)}\right\|_{L^p(\Omega)} \lesssim n^{-\beta} + n^{-\frac{1}{p}} h^{\frac{\sigma p-\theta_*}{p}}, \tag{42}$$

uniformly in $t \in [0, T]$. In both cases the obtained bound is dominated by a constant multiplier of $\mathcal{R}_p(n, h) + h^{\frac{\sigma p-\theta_*}{p}}$. □

6 Simulations

6.1 Simulation of Z

In this section we describe how to simulate the processes $Z_h^{CP,\pm}(t)$. Let us begin with $Z_h^{CP,+}(t)$; as we will see, the procedure for $Z_h^{CP,-}(t)$ is the same.

Let N_t^+ be a time-inhomogeneous Poisson process with integral intensity

$$\lambda_h(t) = \int_0^t \int_{u \ge \tau^+((sh)^\varepsilon)} \nu(du)ds = \int_0^t \left(\frac{1}{hs}\right)^\varepsilon ds = \frac{t^{1-\varepsilon}}{1-\varepsilon}\left(\frac{1}{h}\right)^\varepsilon. \tag{43}$$

Then (cf. [6]) the jump times T_k^+, $k \ge 1$, of N_t^+ can be generated as

$$T_k^+ = (\lambda_h)^{-1}(\Gamma_k), \tag{44}$$

where $\lambda_h^{-1}(t) = \Big(t\,(1-\varepsilon)\,h^\varepsilon\Big)^{\frac{1}{1-\varepsilon}}$ and Γ_k is the jump time of the k-th jump of the Poisson process with intensity 1. Then one can write $Z_h^{CP,+}(t)$ as

$$Z_h^{CP,+}(t) = \sum_{k=1}^{N_t^+} Z_k^+ = \sum_{k\ge 0} Z_k^+ \mathbb{1}_{T_k^+ \le t}, \tag{45}$$

where Z_k^+ is the size of an independent positive jump, occurring at time T_k^+. In this aspect the DC method is crucially different from the AR one, where all jumps have the same distribution. Let us find the distribution of the r.v. Z_k^+.

Denote for simplicity $r_t := \tau^+((ht)^\varepsilon)$. It is shown in [23] that if $\nu(du)$ is absolutely continuous, then the distribution of the jump conditioned by the jump time, occurring at time t, is

$$F_{t,h}^+(x) = \frac{\int_{(r_t, x]} \nu^+(du)}{\int_{(r_t,\infty)} \nu^+(du)} = \frac{N^+(r_t) - N^+(x)}{N^+(r_t)} = 1 - (th)^\varepsilon N^+(x). \tag{46}$$

Then one can simulate Z_k^+ as

$$Z_k^+ \sim (F^+_{T_k^+,h})^{-1}(U) = \tau^+\left(\frac{(T_k^+ h)^{\varepsilon}}{1-U}\right), \qquad U \sim \mathrm{Unif}[0,1]. \tag{47}$$

Note that the integral intensity function corresponding to N^- is again given by (43). Then, in the same way as above we define T_k^-, $F^-_{t,h}$ and Z_k^-, and in such a way we get $Z_h^{CP,-}(t)$, replacing + with − in the respective functions and multiplying the jump sizes by −1.

6.2 Euler-Maruyama approximation

The implementation of the algorithms and simulations of the examples can be found at: GitHub repository.

Algorithm 1 Simulate a single Lévy-type path with omitted small jumps

Require: $T > 0, n \geq 1, x_0 \in \mathbb{R}; h \in (0, h_0], \varepsilon \in (0,1)$
Require: SDE coefficients $a(t,x), b(t,x), c(t,x,z)$
Require: DC functions $\tau^{\pm}(t)$
1: **Get equidistant grid** π_n
2: **Simulate positive and negative jump times** separately via (44) to get $S^{\pm} \subset (0,T]$
3: **Get merged grid** $\Pi = \mathrm{sorted}\left(\{t_k\} \cup \{S^+\} \cup \{S^-\}\right) = \{t_0 < \cdots < t_N\}$
4: **Initialize** $X_{t_0} \leftarrow x_0$
5: **for** $i = 1$ to N **do**
6: $\quad \Delta t \leftarrow t_i - t_{i-1}, \quad x \leftarrow X_{t_{i-1}}$
7: $\quad$ **Drift:** $\Delta X_{\mathrm{drift}} \leftarrow \widetilde{a}(t_{i-1}, t_i, x)\,\Delta t$, cf. (24)
8: $\quad$ **Diffusion:** $\Delta X_{\mathrm{diffusion}} \leftarrow b(t_{i-1}, x)\sqrt{\Delta t}\,\xi$, where $\xi \sim \mathcal{N}(0,1)$
9: $\quad$ **Jumps:** Let $U \sim \mathrm{Unif}(0,1)$, then

$$\Delta X_{\mathrm{jump}} \leftarrow \begin{cases} c(t_i, x, z_i), & \text{if } t_i \in S^{\pm}, \\ 0, & \text{otherwise}. \end{cases}, \quad z_i = \begin{cases} \tau^+\left(\frac{(t_i h)^{\varepsilon}}{1-U}\right), & \text{if } t_i \in S^+, \\ -\tau^-\left(\frac{(t_i h)^{\varepsilon}}{1-U}\right), & \text{if } t_i \in S^-. \end{cases}$$

10: $\quad$ **Update:** $X_{t_i} \leftarrow x + \Delta X_{\mathrm{drift}} + \Delta X_{\mathrm{diffusion}} + \Delta X_{\mathrm{jump}}$
11: **end for**
12: **return** $\{(t_i, X_{t_i})\}_{i=0}^N$

7 Numerical examples and comparisons

We compare the dynamic cutting (DC) scheme with the classical Asmussen–Rosiński (AR) truncation with omitted small jumps in terms of the L^1 – strong error on a purely jump–driven example for $t \in [0,T]$:

$$X_t = \int_0^t \int_{\mathbb{R}} s^{-\sigma} \cos(X_{s-})\, z\, \mathbb{1}_{|z|<1} \widetilde{N}(ds, dz), \qquad X_0 = 0, \tag{48}$$

where $\widetilde{N}$ is the compensated Poisson random measure constructed from the symmetric α-stable Lévy process with Lévy measure $\nu(dz) = \alpha M\,|z|^{-1-\alpha} dz$ with normalization constant $M := \left(2\alpha \int_0^\infty \frac{1-\cos(u)}{u^{1+\alpha}}\, du\right)^{-1}$. In this setting we have $N^{\pm}(r) = \frac{M}{r^\alpha}$ and $\tau^{\pm}(t) = (Mt)^{1/\alpha}$.

7.1 Time complexity analysis of a pure-jump process

We consider the case of a pure-jump process, where the drift and diffusion coefficients are zero. In this scenario, the simulation algorithm is simplified, as the process state is constant between jumps. The time grid is constructed solely from the jump times.

The algorithm first simulates the times and sizes of all large jumps up to the horizon T. The jump times for the positive and negative jumps are then merged and sorted to create a chronologically ordered list. The computational bottleneck of this step is the sorting of two ordered arrays, which has a complexity of $O(N)$, where N is the length of that sorted list.

The algorithm then iterates once through the sorted list of N jumps. At each jump, it updates the process state by applying the jump coefficient. This step involves a single pass resulting in a complexity of order $O(N)$.

It is crucial to note that this complexity analysis holds for both AR and DC methods. The underlying functions that distinguish these methods, such as λ_h^{-1} and $(F^{\pm})^{-1}$, are compositions of elementary operations and are executed in constant time $O(1)$. Thus, the choice between AR and DC does not change the overall asymptotic complexity of the simulation as long as N is equal.

Remark 7.1. Instead of using the approach (44), one can simulate the ICPP by thinning (cf. [19]), i.e. simulate the jumps of the Poisson process with dominating (e.g., piecewise constant) intensity, and accept each candidate with probability proportional to the target intensity in both the AR and DC methods. The type of jump (positive or negative) is then assigned to each accepted time. This construction produces jump times directly in chronological order and has (up to a multiplicative constant) the same order of computational complexity (possibly with another multiplicative constant).

Remark 7.2. Let us compare our result with that from [7]. In our case for the DC scheme we have

$$\mathbb{E}[\mathrm{cost}] = \mathbb{E}[N_h] = 2\lambda_h(T) = \frac{2T^{1-\varepsilon}}{1-\varepsilon}\, h^{-\varepsilon},$$

so the expected computational cost satisfies $O(h^{-\varepsilon})$.

Now let $h = h(n)$ be chosen so that the strong error bound in Theorem 3.1 preserves the leading rate $n^{-\beta}$, i.e. h is as in (30). Substituting this into $h^{-\varepsilon}$ yields

$$\mathbb{E}[\mathrm{cost}] = \begin{cases} O\left(n^{\frac{\beta\alpha p}{p-\alpha}}\right), & p < 2, \\ O\left(n^{\frac{2\beta\alpha}{2-\alpha}}\right), & p \geq 2. \end{cases}$$

In particular, for $p = 2$ and $\beta = \frac{1}{2}$ one obtains $O\left(n^{\frac{\alpha}{2-\alpha}}\right)$, which coincides with the classical complexity, see, for example, Fournier [7].

7.2 Comparison of AR and DC

For simplicity, take $T = 1$, and suppose that the expected number of simulated jumps on $[0, 1]$ is fixed. We compare AR and DC at matched time complexity. Since we consider a pure-jump case, it is sufficient to make this number equal for both schemes.

Denote by $\mathcal{NJ}$ the number of jumps, expected in both schemes. For AR with a fixed threshold $\delta_{\text{AR}} \in (0,1)$, the expected number of retained jumps on $[0,1]$ equals

$$\mathcal{NJ} = N(\delta_{\text{AR}}) = \frac{2M}{\delta_{\text{AR}}^{\alpha}} \quad \Longrightarrow \quad \delta_{\text{AR}} = \left(\frac{2M}{\mathcal{NJ}}\right)^{1/\alpha}. \tag{49}$$

For DC with parameters h and ε, by equation (43), the expected number of retained jumps on $[0,1]$ is

$$\mathcal{NJ} = 2\lambda_h(1) = \frac{2}{1-\varepsilon}\, h^{-\varepsilon} \quad \Longrightarrow \quad h = \left(\frac{\mathcal{NJ}\,(1-\varepsilon)}{2}\right)^{-1/\varepsilon}. \tag{50}$$

We still have one undefined parameter ε. To choose some reasonable value, we consider the variance of additive process

$$\widetilde{Z}_t^{(h,\varepsilon)} = \int_0^t \int_{B(s,h)} s^{-\sigma} z \widetilde{N}(ds, dz).$$

Now fixing $\mathcal{NJ}$ we find the ε, which minimizes the variance of $\widetilde{Z}_t$:

$$J^{DC}(\varepsilon) := \operatorname{Var} \widetilde{Z}_t^{(h,\varepsilon)} = 2\int_0^1 \int_0^{\tau((sh)^{\varepsilon})} s^{-2\sigma} z^2\, \nu(dz) ds.$$

The above integral can be calculated explicitly and minimized w.r.t. ε:

$$\arg\min_{\varepsilon} J^{DC}(\varepsilon) = \alpha\sigma. \tag{51}$$

Thus, we set $\varepsilon_\star = \alpha/4$ (cf. (48)).

We define two trajectory versions based on the expected number of jumps: a fine level ($\mathcal{NJ}^{\text{fine}} = 64{,}000$ jumps) and a coarse level ($\mathcal{NJ}^{\text{coarse}} = 4{,}000$ jumps). For each level we determine two sets of simulation parameters using equations (49) and (50):

1. **Fine parameters:** $(\delta_{\text{AR}}^{\text{fine}}, h^{\text{fine}})$, by taking $\mathcal{NJ} = \mathcal{NJ}^{\text{fine}}$.
2. **Coarse parameters:** $(\delta_{\text{AR}}^{\text{coarse}}, h^{\text{coarse}})$, by taking $\mathcal{NJ} = \mathcal{NJ}^{\text{coarse}}$.

To couple the simulations, we first generate a single *fine* path using the fine parameters. We then derive the *coarse* path by filtering the jumps from this fine path using the coarse parameters. The coupling procedure is as follows:

1. Generate a single *fine* path on $[0,1]$ with an expected $\mathcal{NJ}^{\text{fine}}$ jumps, using the calculated $(\delta_{\text{AR}}^{\text{fine}}, h^{\text{fine}})$ parameters.
2. From this fine path, build a *coarse* path by retaining a jump at time s only if it exceeds the coarse-level threshold:
   - **DC method:** The jump is kept if $|z| \geq \tau\big((sh^{\text{coarse}})^{\varepsilon}\big)$.
   - **AR method:** The jump is kept if $|z| \geq \delta_{\text{AR}}^{\text{coarse}}$.

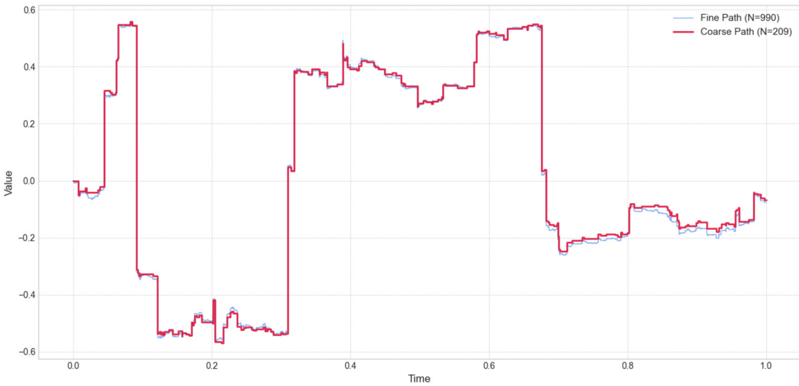

Fig. 3. Illustration of the coupled construction ($\mathcal{NJ}^{\text{fine}} = 1000$, $\mathcal{NJ}^{\text{coarse}} = 200$)

This coupling ensures that fine and coarse trajectories are not completely independent, but built based on the same underlying randomness.

Let $Y := \sup_{0\le t\le 1} \left|X_t^{\text{fine}} - X_t^{\text{coarse}}\right|$, and define i.i.d. copies

$$Y_k = \sup_{0\le t\le 1} \left|X_t^{\text{fine},(k)} - X_t^{\text{coarse},(k)}\right|, \qquad 1 \le k \le D.$$

We apply the CLT to the i.i.d. sequence $(Y_k)_{k\ge1}$, which requires $\mathbb{E}Y_k^2 < \infty$. From (48), $\mathbb{E}Y^2 < \infty$ provided that $\sigma < 1/2$, for both the AR and DC methods. Let $\overline{Y} := \frac{1}{D}\sum_{k=1}^D Y_k$ and $s_Y^2 := \frac{1}{D-1}\sum_{k=1}^D (Y_k - \overline{Y})^2$. By the delta method with $g(x) = \sqrt{x}$, we obtain the standard error $\widehat{\text{SE}}\left(\sqrt{\overline{Y}}\right) = \frac{s_Y}{2\sqrt{D}\sqrt{\overline{Y}}}$. Thus,

$$\left[\left(\sqrt{\overline{Y}} - 1.96\,\widehat{\text{SE}}\left(\sqrt{\overline{Y}}\right)\right)^2, \left(\sqrt{\overline{Y}} + 1.96\,\widehat{\text{SE}}\left(\sqrt{\overline{Y}}\right)\right)^2\right]$$

is the asymptotic 95% confidence interval for $\mathbb{E}Y$. The Monte Carlo simulations were performed with $D = 10{,}000$ replications. We considered three distinct groups of values for α:

1. **Small values:** $\alpha \in \{0.1, 0.2, 0.3, 0.4\}$
2. **Middle values:** $\alpha \in \{0.5, 1.0, 1.5\}$
3. **Large values:** $\alpha \in \{1.6, 1.7, 1.8, 1.9\}$

Under matched time complexity, DC consistently gives slightly smaller L^1 errors when the jump coefficient has early-time singularity $c(t,\cdot,\cdot) \lesssim t^{-\sigma}$ with $\sigma > 0$. We take $p = 2$, and observe that (14) is satisfied, if $\sigma < 1/p = 0.5$. We observe that for σ close to 0.5 DC outperforms AR for all tested α, with the largest relative gains at small α. AR's time-uniform cutoff δ_{AR} discards all $|z| < \delta_{\text{AR}}$, removing early small jumps whose contribution is magnified by the weight $s^{-\sigma}$. DC lowers its cutoff near $t = 0$ and retains these jumps, producing a bigger gap in favor of DC at small α.

Table 2. Comparison of simulation results for AR and DC ($\sigma = 0.25$)

	AR Method			DC Method		
		95% CI			95% CI	
α	**Error**	**Lower**	**Upper**	**Error**	**Lower**	**Upper**
			Small α			
0.10	4.952e−36	3.789e−36	6.270e−36	**2.657e−36**	7.878e−37	5.628e−36
0.20	2.025e−17	1.988e−17	2.063e−17	**1.614e−17**	1.581e−17	1.648e−17
0.30	2.750e−11	2.726e−11	2.773e−11	**2.470e−11**	2.449e−11	2.491e−11
0.40	3.317e−08	3.289e−08	3.346e−08	**2.968e−08**	2.942e−08	2.994e−08
			Middle α			
0.50	2.434e−06	2.413e−06	2.455e−06	**2.172e−06**	2.153e−06	2.192e−06
1.00	1.582e−02	1.566e−02	1.598e−02	**1.413e−02**	1.398e−02	1.428e−02
1.50	2.884e−01	2.850e−01	2.919e−01	**2.644e−01**	2.613e−01	2.676e−01
			Large α			
1.60	3.938e−01	3.889e−01	3.986e−01	**3.665e−01**	3.620e−01	3.709e−01
1.70	4.978e−01	4.919e−01	5.037e−01	**4.698e−01**	4.642e−01	4.755e−01
1.80	5.766e−01	5.700e−01	5.832e−01	**5.529e−01**	5.466e−01	5.592e−01
1.90	5.751e−01	5.693e−01	5.810e−01	**5.618e−01**	5.560e−01	5.676e−01

7.3 Removing the time-singularity

To verify that the performance gap observed in the main experiment is driven by the time-decay in the jump coefficient, we repeat the simulation with the factor $s^{-\sigma}$ removed from $c(t,x,z)$. In (51) we selected ε by minimizing a proxy for the small-jump variance, which yields $\varepsilon_\star = \alpha\sigma$. For $\sigma = 0$ this collapses to $\varepsilon_\star = 0$, producing a degenerate DC cutoff. Therefore, we fix a small, strictly positive constant $\varepsilon = 0.1$ for all α, and re-tune h to keep the expected number of retained jumps as before. The rest of the setup remains the same.

$$X_t = \int_0^t \int_{\mathbb{R}} \cos(X_{s-})\, \mathbb{1}_{\{|z|\le 1\}}\, z\, \widetilde{N}(ds,dz), \qquad t \in [0,1], \quad X_0 = 0,$$

The obtained results can be observed in Table 3. In this setting ($\sigma = 0$), neither method has a uniform advantage.

7.4 Extreme time-singularity

We also examine the extreme case where $\sigma = 0.4999$, a value approaching the critical threshold of 0.5, to highlight the performance disparity between the two approaches. The results are summarized in Table 4. As we see from the table, the difference between the outcomes of two methods is more visible for small α, and narrows as α approaches 2.

7.5 Synthetic example

Finally, consider a "synthetic" example, which highlights the impact of small jumps, when the intensity of jumps is low. Consider a symmetric α-stable Lévy measure and take

$$c(t,x,z) = z\cos(x)\, t^{-\sigma}\, \mathbb{1}\{t^{1/\alpha} \le |z| \le C\, t^{1/\alpha}\}, \tag{52}$$

with $\sigma = 0.6$ and $C = 10$. Thus, the singular activity is concentrated on the floating window $[t^{1/\alpha}, Ct^{1/\alpha}]$, which slides towards 0 as $t \to 0$. In Table 5 we present the

Table 3. Comparison of simulation results for AR and DC ($\sigma = 0$)

α	AR Method Error	AR 95% CI Lower	AR 95% CI Upper	DC Method Error	DC 95% CI Lower	DC 95% CI Upper
			Small α			
0.10	1.380e−36	8.257e−37	2.075e−36	**1.028e−37**	7.237e−39	3.094e−37
0.20	1.260e−17	1.236e−17	1.285e−17	**1.200e−17**	1.176e−17	1.224e−17
0.30	**1.958e−11**	1.942e−11	1.974e−11	2.090e−11	2.072e−11	2.107e−11
0.40	**2.365e−08**	2.345e−08	2.384e−08	2.444e−08	2.424e−08	2.465e−08
			Middle α			
0.50	**1.736e−06**	1.722e−06	1.751e−06	1.769e−06	1.754e−06	1.784e−06
1.00	1.124e−02	1.113e−02	1.134e−02	**1.120e−02**	1.110e−02	1.130e−02
1.50	2.040e−01	2.020e−01	2.060e−01	**2.031e−01**	2.010e−01	2.051e−01
			Large α			
1.60	2.798e−01	2.770e−01	2.826e−01	**2.791e−01**	2.763e−01	2.819e−01
1.70	3.568e−01	3.532e−01	3.603e−01	**3.559e−01**	3.524e−01	3.594e−01
1.80	4.177e−01	4.137e−01	4.218e−01	**4.169e−01**	4.129e−01	4.210e−01
1.90	4.206e−01	4.168e−01	4.244e−01	**4.203e−01**	4.165e−01	4.241e−01

Table 4. Comparison of simulation results for AR and DC ($\sigma = 0.4999$)

α	AR Method Error	AR 95% CI Lower	AR 95% CI Upper	DC Method Error	DC 95% CI Lower	DC 95% CI Upper
			Small α			
0.10	3.999e−35	2.238e−35	6.267e−35	**2.486e−36**	1.411e−36	3.864e−36
0.20	5.499e−17	5.406e−17	5.593e−17	**2.090e−17**	2.047e−17	2.133e−17
0.30	6.973e−11	6.881e−11	7.066e−11	**3.207e−11**	3.179e−11	3.235e−11
0.40	8.710e−08	8.594e−08	8.827e−08	**3.875e−08**	3.840e−08	3.911e−08
			Middle α			
0.50	6.631e−06	6.540e−06	6.723e−06	**2.869e−06**	2.841e−06	2.896e−06
1.00	5.488e−02	5.370e−02	5.607e−02	**2.130e−02**	2.100e−02	2.160e−02
1.50	1.168e+00	1.145e+00	1.192e+00	**5.842e−01**	5.711e−01	5.973e−01
			Large α			
1.60	1.520e+00	1.489e+00	1.550e+00	**8.505e−01**	8.319e−01	8.694e−01
1.70	1.794e+00	1.759e+00	1.828e+00	**1.123e+00**	1.099e+00	1.147e+00
1.80	1.942e+00	1.906e+00	1.979e+00	**1.361e+00**	1.333e+00	1.390e+00
1.90	1.810e+00	1.777e+00	1.842e+00	**1.519e+00**	1.490e+00	1.548e+00

L^1 – strong errors for $\alpha \in [0.1, 1.6]$ using $D = 10,000$ Monte Carlo simulations and matching computational cost between AR and DC.

Heuristically, for the α-stable case with $c(t, x, z)$ as above, the second-moment contribution within the given window scales as

$$\int t^{-2\sigma}\Big(\int_{t^{1/\alpha}}^{Ct^{1/\alpha}} z^2\,\nu(dz)\Big)\,dt \;\asymp\; \int t^{-2\sigma+(2-\alpha)/\alpha}\,dt,$$

which leads to the integrability condition $\alpha\sigma < 1$, which is more relaxed than $\sigma p < 1$. With $\sigma = 0.6$ this yields the critical value $\alpha \approx 1/\sigma \approx 1.66$. Table 5 reflects this boundary: DC remains good up to $\alpha = 1.5$ but increases sharply at $\alpha = 1.6$ as $\alpha\sigma \uparrow 1$.

Overall, Table 5 demonstrates significantly lower errors for the DC approach.

Table 5. Comparison of L^1 strong errors for synthetic example

α	AR Method Error	AR Method 95% CI	DC Method Error	DC Method 95% CI
0.10	1.86×10^{-36}	$[1.69, 2.05] \times 10^{-36}$	$\mathbf{2.08 \times 10^{-38}}$	$[1.88, 2.29] \times 10^{-38}$
0.20	8.68×10^{-18}	$[8.10, 9.28] \times 10^{-18}$	$\mathbf{1.13 \times 10^{-19}}$	$[0.957, 1.32] \times 10^{-19}$
0.30	1.72×10^{-11}	$[1.66, 1.78] \times 10^{-11}$	$\mathbf{1.78 \times 10^{-13}}$	$[1.71, 1.86] \times 10^{-13}$
0.40	3.18×10^{-8}	$[3.08, 3.28] \times 10^{-8}$	$\mathbf{3.07 \times 10^{-10}}$	$[2.94, 3.20] \times 10^{-10}$
0.50	3.26×10^{-6}	$[3.16, 3.36] \times 10^{-6}$	$\mathbf{3.00 \times 10^{-8}}$	$[2.89, 3.11] \times 10^{-8}$
0.60	7.75×10^{-5}	$[7.49, 8.01] \times 10^{-5}$	$\mathbf{6.92 \times 10^{-7}}$	$[6.70, 7.15] \times 10^{-7}$
0.70	7.83×10^{-4}	$[7.57, 8.09] \times 10^{-4}$	$\mathbf{6.74 \times 10^{-6}}$	$[6.55, 6.95] \times 10^{-6}$
0.80	4.96×10^{-3}	$[4.45, 5.49] \times 10^{-3}$	$\mathbf{3.90 \times 10^{-5}}$	$[3.79, 4.02] \times 10^{-5}$
0.90	1.94×10^{-2}	$[1.88, 2.01] \times 10^{-2}$	$\mathbf{1.64 \times 10^{-4}}$	$[1.59, 1.70] \times 10^{-4}$
1.00	6.17×10^{-2}	$[5.94, 6.40] \times 10^{-2}$	$\mathbf{5.51 \times 10^{-4}}$	$[5.26, 5.76] \times 10^{-4}$
1.10	1.64×10^{-1}	$[1.57, 1.72] \times 10^{-1}$	$\mathbf{1.51 \times 10^{-3}}$	$[1.46, 1.56] \times 10^{-3}$
1.20	3.72×10^{-1}	$[3.58, 3.86] \times 10^{-1}$	$\mathbf{3.90 \times 10^{-3}}$	$[3.69, 4.11] \times 10^{-3}$
1.30	6.95×10^{-1}	$[6.73, 7.18] \times 10^{-1}$	$\mathbf{9.75 \times 10^{-3}}$	$[9.10, 10.4] \times 10^{-3}$
1.40	1.11	$[1.08, 1.14]$	$\mathbf{2.40 \times 10^{-2}}$	$[2.25, 2.56] \times 10^{-2}$
1.50	1.61	$[1.57, 1.65]$	$\mathbf{7.68 \times 10^{-2}}$	$[7.16, 8.22] \times 10^{-2}$
1.60	2.08	$[2.02, 2.13]$	$\mathbf{4.58 \times 10^{-1}}$	$[4.34, 4.82] \times 10^{-1}$

8 Conclusion

Under matched time complexity, the DC scheme achieves consistently but slightly smaller L^1 errors (see Table 2) when the jump coefficient $c(t, x, z)$ has an early-time singularity with $\sigma > 0$. DC's time-dependent threshold retains more early small-size jumps that a fixed AR cutoff misses, which demonstrates most clearly when the small-jump intensity is low. In a control run with the time singularity removed ($\sigma = 0$), neither method has a uniform advantage (see Table 3). Within the examples considered above, DC produced smaller errors when the time-decaying jump coefficient was singular at $t = 0$ under the matched-cost regime of equal expected retained-jump counts. Note that in these experiments we choose ε heuristically, aiming to reduce the variance of the omitted small-jump component near the singularity. We plan to analyze this problem of the optimal choice in forthcoming research.

A Auxiliary lemmas

We begin with quoting the following estimate on $\tau(t)$.

Lemma A.1 ([9, Lem. 4.3])**.** *For any $R > 1$, there exists a constant $w > 0$ such that*

$$\tau(Rt) \le R^w \tau(t) \quad \textit{for all } t > 0.$$

Corollary A.2. *Since $\tau(t)$ is strictly non-decreasing, taking $R = \max\{2, T^\varepsilon\}$ in Lemma A.1, for any $h, \varepsilon \in (0, 1)$ we derive*

$$\tau((th)^\varepsilon) \lesssim \tau(h^\varepsilon), \quad t \in [0, T].$$

Lemma A.3. *For any $p \ge 2$,*

$$\int_{B(s,h)} |c(s, x, z)|^p \ \nu(dz) \lesssim (1 + |x|)^p s^{-p\sigma} \frac{\big(\tau((sh)^\varepsilon)\big)^p}{(sh)^\varepsilon}.$$

Proof. For $p \geq 2$, using (18) and definition (7) of ψ^L, we derive

$$\begin{aligned}
\int_{B(s,h)} |c(s,x,z)|^p \, \nu(dz) &\lesssim (1+|x|)^p s^{-p\sigma} \int_{B(s,h)} |z|^p \, \nu(dz) \\
&\leq (1+|x|)^p (\tau^+((sh)^\varepsilon))^p s^{-p\sigma} \int_0^{\tau^+((sh)^\varepsilon)} |(\tau^+((sh)^\varepsilon))^{-1} z|^p \, \nu(dz) \\
&\quad + (1+|x|)^p (\tau^-((sh)^\varepsilon))^p s^{-p\sigma} \int_{-\tau^-((sh)^\varepsilon)}^0 |(\tau^-((sh)^\varepsilon))^{-1} z|^p \, \nu(dz) \\
&\leq (1+|x|)^p \tau^p((sh)^\varepsilon) s^{-p\sigma} \int_0^{\tau^+((sh)^\varepsilon)} |(\tau^+((sh)^\varepsilon))^{-1} z|^2 \, \nu(dz) \\
&\quad + (1+|x|)^p \tau^p((sh)^\varepsilon) s^{-p\sigma} \int_{-\tau^-((sh)^\varepsilon)}^0 |(\tau^-((sh)^\varepsilon))^{-1} z|^2 \, \nu(dz).
\end{aligned}$$

Since $\psi^{L,\pm}(1/\xi) \lesssim N^\pm(\xi)$, $\xi \in (0,1)$ (cf. Assumption 1), we obtain

$$\begin{aligned}
\int_{B(s,h)} |c(s,x,z)|^p \, \nu(dz) &\lesssim (1+|x|)^p s^{-p\sigma} \tau^p((sh)^\varepsilon) \\
&\quad \cdot \left[N^+\big(\tau^+((sh)^\varepsilon)\big) + N^+\big(\tau^+((sh)^\varepsilon)\big)\right] \\
&= (1+|x|)^p s^{-p\sigma} \tau^p((sh)^\varepsilon)(sh)^{-\varepsilon}. \qquad \square
\end{aligned}$$

In the next lemma we formulate the general result, which will be needed in several proofs.

Lemma A.4. *Let $m(\cdot)$ be some measure on $\mathcal{B}(\mathbb{R})$, $a > 0$. Assume that $M(u) := m(|z| > u) \lesssim u^{-a}$ for $u \in (0,1]$. Then for any $q > a$ and $R \in (0,1]$:*

$$\int_{|z|<R} |z|^q m(dz) \lesssim \frac{q}{q-a} R^{q-a}.$$

Proof. For $q > 0$,

$$|z|^q \mathbb{1}_{\{|z|<R\}} = \int_0^R q u^{q-1} \mathbb{1}_{\{u<|z|<R\}} \, du \leq \int_0^R q u^{q-1} \mathbb{1}_{\{|z|>u\}} \, du.$$

Integrating w.r.t. $m(dz)$ and applying the Fubini theorem, we get

$$\int_{|z|<R} |z|^q m(dz) \leq q \int_0^R u^{q-1} M(u) \, du \lesssim q \int_0^R u^{q-1} u^{-a} \, du = \frac{q}{q-a} R^{q-a}. \quad \square$$

Lemma A.5. *Let $\alpha \in (0,2)$ be from (9). Then, for any $p > \alpha$, we have*

$$\int_{B(s,h)} |c(s,x,z)|^p \, \nu(dz) \lesssim (1+|x|)^p s^{-p\sigma} \tau^{p-\alpha}((sh)^\varepsilon).$$

Proof. Note that $B(s,h) \subset \widetilde{B}(s,h) := \big\{z : |z| < \tau((sh)^\varepsilon)\big\}$. Using (18) and the Fubini-Tonelli theorem, we obtain

$$\int_{B(s,h)} |c(s,x,z)|^p \, \nu(dz) \lesssim (1+|x|)^p s^{-p\sigma} \int_{B(s,h)} |z|^p \, \nu(dz)$$

$$\leq (1+|x|)^p s^{-p\sigma} \int_{\widetilde{B}(s,h)} |z|^p\, \nu(dz) \lesssim (1+|x|)^p s^{-p\sigma} \tau^{p-\alpha}((sh)^\varepsilon),$$

where in the last inequality we used Lemma A.4. □

Lemma A.6. *Let $p \geq 2$. Then*

i) if $p\sigma + \varepsilon < 1$, then

$$\mathbb{E} \int_0^t \int_{B(s,h)} \left|c(s, X_s, z)\right|^p \nu(dz)\, ds \lesssim \tau^p(h^\varepsilon) h^{-\varepsilon};$$

ii) if $p\sigma + \varepsilon < 1 + \varepsilon p/\alpha$, then

$$\mathbb{E} \int_0^t \int_{B(s,h)} \left|c(s, X_s, z)\right|^p \nu(dz) ds \lesssim h^{\frac{\varepsilon(p-\alpha)}{\alpha}}.$$

Proof. We use Lemma A.3, Corollary A.2 to Lemma A.1, and Remark 2.3, which ensures the existence of moments $\mathbb{E}^x \sup_{s\in[0,t]} |X_s|^p \leq C(x)$; here the constant $C(x)$ depends on the starting point x. Then

$$\begin{aligned}
\mathbb{E} \int_0^t \int_{B(s,h)} \left|c(s, X_s, z)\right|^p \nu(dz)\, ds &\lesssim \mathbb{E} \int_0^t \left(1+|X_s|\right)^p s^{-p\sigma} \frac{\tau^p((sh)^\varepsilon)}{(sh)^\varepsilon}\, ds \\
&\lesssim \tau^p(h^\varepsilon) h^{-\varepsilon} \int_0^t \mathbb{E}\left(1+|X_s|\right)^p s^{-p\sigma-\varepsilon}\, ds \\
&\lesssim \tau^p(h^\varepsilon) h^{-\varepsilon}\, \mathbb{E} \sup_{s\in[0,t]} \left(1+|X_s|\right)^p \int_0^t s^{-p\sigma-\varepsilon}\, ds \\
&\lesssim \tau^p(h^\varepsilon) h^{-\varepsilon},
\end{aligned}$$

provided that $p\sigma + \varepsilon < 1$. This proves i). To show ii), we estimate $\tau((sh)^\varepsilon)$ on the earlier stage, provided that $p(\varepsilon/\alpha - \sigma) + 1 - \varepsilon > 0$:

$$\mathbb{E} \int_0^t \int_{B(s,h)} \left|c(s, X_s, z)\right|^p \nu(dz)\, ds \lesssim \int_0^t (sh)^{\varepsilon p/\alpha - \varepsilon} s^{-\sigma p} ds \lesssim h^{\frac{\varepsilon(p-\alpha)}{\alpha}}. \quad \square$$

Lemma A.7 (Strong convergence of the adapted Euler-Peano scheme)**.** *Under the assumptions of Theorem 3.1, for any $h \in (0, h_0]$,*

$$\left\| \sup_{t\in[0,T]} |X_t - \widetilde{X}_t| \right\|_{L^p(\Omega)} \lesssim \mathcal{R}_p(n,h), \tag{53}$$

where $\mathcal{R}_p(n,h) = n^{-\beta} + \mathfrak{r}_p(n,h)$,

$$\mathfrak{r}_p(n,h) := \begin{cases} n^{-\frac{\kappa}{p}} h^{\frac{2(\sigma p - \theta_*)}{p}} (1 + \mathbb{1}_{\{\theta_* = \frac{1}{2}\}} \ln n), & p < 2, \\ n^{-\frac{1}{p}} h^{\frac{\sigma p - \theta_*}{p}} + n^{-\frac{\kappa}{p}} h^{\frac{2(\sigma p - \theta_*)}{p}} (1 + \mathbb{1}_{\{\theta_* = \frac{1}{2}\}} \ln n), & p \geq 2, \end{cases}$$

and $\beta = \min(\gamma, 1/2, 1-\chi)$, $\kappa = \min(1, 2(1-\theta_*))$.

Corollary A.8. *By choosing h sufficiently small such that $h^{\sigma p-\theta_*} \lesssim 1$ (which is possible since $p\sigma - \theta_* > 0$), we obtain the simplified rate:*

$$\left\| \sup_{t\in[0,T]} |X_t - \widetilde{X}_t| \right\|_{L^p(\Omega)} \lesssim n^{-\beta_0}, \tag{54}$$

where

$$\beta_0 = \begin{cases} \min\left\{\gamma, \frac{1}{2}, \frac{\kappa}{p}, 1-\chi\right\}, & p < 2, \\ \min\left\{\gamma, \frac{1}{p}, \frac{\kappa}{p}, 1-\chi\right\}, & p \geq 2. \end{cases}$$

Proof. We conduct both cases a) and b) of Theorem 3.1 parallel, indicating the changes in the proof. We distinguish two cases $p < 2$ and $p \geq 2$, having in mind that p belongs to the intervals, defined in Theorem 3.1.

Set $\mathcal{E}_t := |X_t - \widetilde{X}_t|$ and $f(t) := \| \sup_{s\in[0,t]} \mathcal{E}_s \|_{L^p(\Omega)}$. Applying the triangle inequality, we get

$$\begin{aligned} f(t) &\leq \left\| \sup_{s\leq t} \left| \int_0^s \left(a(u, X_u) - a(\eta(u), \widetilde{X}_{\eta(u)}) \right) du \right| \right\|_{L^p(\Omega)} \\ &+ \left\| \sup_{s\leq t} \left| \int_0^s \left(b(u, X_u) - b(\eta(u), \widetilde{X}_{\eta(u)}) \right) dB_u \right| \right\|_{L^p(\Omega)} \\ &+ \left\| \sup_{s\leq t} \left| \int_0^s \int_{-\infty}^{+\infty} \left(c(u, X_{u-}, z) - c(u, \widetilde{X}_{\eta(u-)}, z) \right) \widetilde{N}(du, dz) \right| \right\|_{L^p(\Omega)} \\ &=: \mathbf{(A)} + \mathbf{(B)} + \mathbf{(C)}. \end{aligned}$$

We now bound each of the three terms on the right-hand side.

The Drift component. Using Minkowski's integral inequality, Lipschitz and Peano assumptions (11) and (16), boundedness of moments of X_u (cf. Remark 2.3), the triangle inequality and that $0 \leq u - \eta(u) \leq T/n$, we derive

$$\begin{aligned} \mathbf{(A)} &\leq \int_0^t \left\| a(u, X_u) - a(\eta(u), \widetilde{X}_{\eta(u)}) \right\|_{L^p(\Omega)} du \\ &\lesssim \frac{T^{\gamma+1}}{n^\gamma} + \int_0^t f(s) ds + \int_0^t \left\| \widetilde{X}_s - \widetilde{X}_{\eta(s)} \right\|_{L^p(\Omega)} ds. \end{aligned}$$

Since $s - \eta(s) \lesssim n^{-1}$, in the time interval $[\eta(s), s]$ we have only jumps of size $B(r, h)$, which allows us to write

$$\begin{aligned} \widetilde{X}_s - \widetilde{X}_{\eta(s)} &= a(\eta(s), \widetilde{X}_{\eta(s)})(s - \eta(s)) + b(\eta(s), \widetilde{X}_{\eta(s)})(B_s - B_{\eta(s)}) \\ &\quad + \int_{\eta(s)}^s \int_{B(r,h)} c(r, \widetilde{X}_{\eta(r-)}, z) \widetilde{N}(dr, dz) \\ &\quad - \int_{\eta(s)}^s \int_{B^c(r,h)} c(r, \widetilde{X}_{\eta(r-)}, z) \nu(dz)\, dr := \sum_{k=1}^4 I_k, \end{aligned}$$

We first obtain the estimate on the local increment $\|\widetilde{X}_s - \widetilde{X}_{\eta(s)}\|_{L^p}$. Since $s - \eta(s) \lesssim n^{-1}$, the upper bound on the L^p – norms of the first two terms are of order n^{-1} and $n^{-1/2}$, respectively. For I_3 we first bound the integral from above as

$$\left|\int_{\eta(s)}^{s} \int_{B(r,h)} c(r, \widetilde{X}_{\eta(r-)}, z)\, \widetilde{N}(dr, dz)\right| \\ \leq \sup_{\chi \in [(s-\Delta)_+, s]} \left|\int_{\chi}^{s} \int_{B(r,h)} c(r, \widetilde{X}_{\eta(r-)}, z)\, \widetilde{N}(dr, dz)\right|.$$

Then we can apply (18), Kunita's (for $p \geq 2$) or Novikov's ($p < 2$) BDG inequality:

$$\left\|\int_{\eta(s)}^{s} \int_{B(r,h)} c(r, \widetilde{X}_{\eta(r-)}, z) \widetilde{N}(dr, dz)\right\|_{L^p(\Omega)} \lesssim \left(\int_{(s-\Delta)_+}^{s} m_p(r) dr\right)^{1/p}, \tag{55}$$

where $\Delta := T/n$, $m_p(r) := r^{-p\sigma} h_p(r)$, and

$$h_p(r) := \begin{cases} \int_{B(r,h)} |z|^p \nu(dz), & p < 2, \\ \left(\int_{B(r,h)} |z|^2 \nu(dz)\right)^{p/2} + \int_{B(r,h)} |z|^p \nu(dz), & p \geq 2. \end{cases}$$

Let us estimate I_4. If (19) is satisfied, this term is equal to 0. In the case of (20), we get

$$\left\|\int_{\eta(s)}^{s} \int_{B^c(r,h)} c(r, \widetilde{X}_{\eta(r-)}, z) \nu(dz)\, dr\right\|_{L^p(\Omega)} \lesssim \int_{\eta(s)}^{s} M_{1,h}(r)\, dr \lesssim n^{-1+\chi} \lesssim n^{-\beta}.$$

Thus,

$$\|\widetilde{X}_s - \widetilde{X}_{\eta(s)}\|_{L^p} \lesssim n^{-\beta} + \left(\int_{(s-\Delta)_+}^{s} m_p(r)\, dr\right)^{1/p}. \tag{56}$$

Let $g(s) := \int_{(s-\Delta)_+}^{s} m_p(r) dr$. Application of Hölder's inequality on $[0, t]$ with exponents p and $p/(p-1)$ yields

$$\int_0^t g^{\frac{1}{p}}(s)\, ds \leq \left(\int_0^t 1^{\frac{p}{p-1}} ds\right)^{\frac{p-1}{p}} \left(\int_0^t g(s) ds\right)^{1/p} = t^{1-1/p} \left(\int_0^t g(s)\, ds\right)^{1/p}.$$

Using Fubini's theorem we arrive at

$$\int_0^t \left\|\widetilde{X}_s - \widetilde{X}_{\eta(s)}\right\|_{L^p(\Omega)} ds \lesssim t\, n^{-\beta} + t^{1-1/p} \left(n^{-1} \int_0^t m_p(r) dr\right)^{1/p}. \tag{57}$$

Using Lemmas A.3, A.5 and the estimate $\tau(t) \lesssim t^{1/\alpha}$, cf. (8), we get

$$h_p(r) \lesssim \begin{cases} (rh)^{\frac{(p-\alpha)\varepsilon}{\alpha}}, & p < 2 \\ (rh)^{\frac{(2-\alpha)\varepsilon p}{2\alpha}} + (rh)^{\frac{(p-\alpha)\varepsilon}{\alpha}}, & p \geq 2. \end{cases} \tag{58}$$

Thus, under the assumptions on σ in Theorem 3.1, in both cases a) or b) of this theorem, we have

$$m_p(r) \lesssim \begin{cases} h^{\frac{\varepsilon(p-\alpha)}{\alpha}} r^{-\theta_*}, & p < 2, \\ h^{\frac{\varepsilon p(2-\alpha)}{2\alpha}} r^{-\theta_*}, & p \geq 2, \end{cases} \tag{59}$$

$$\int_{(t-\Delta)_+}^t m_p(s)ds \lesssim h^{\sigma p-\theta_*} t^{-\theta_*}\Delta, \quad \int_0^t m_p(s)ds \lesssim h^{\sigma p-\theta_*} t^{1-\theta_*}, \tag{60}$$

where the last estimate follows from $\theta_* < (\zeta-1)/\zeta < 1$. Consequently, in both cases of Theorem 3.1,

$$\left\| \widetilde{X}_s - \widetilde{X}_{\eta(s)} \right\|_{L^p(\Omega)} \lesssim n^{-\beta} + n^{-\frac{1}{p}} h^{\frac{\sigma p-\theta_*}{p}} s^{-\frac{\theta_*}{p}}, \tag{61}$$

$$\int_0^t \left\| \widetilde{X}_s - \widetilde{X}_{\eta(s)} \right\|_{L^p(\Omega)} ds \lesssim n^{-\beta} + n^{-\frac{1}{p}} h^{\frac{\sigma p-\theta_*}{p}}. \tag{62}$$

Thus,

$$\mathbf{(A)} \lesssim \begin{cases} n^{-\beta} + \int_0^t f(s)ds, & p < 2, \\ n^{-\beta} + n^{-\frac{1}{p}} h^{\frac{\sigma p-\theta_*}{p}} + \int_0^t f(s)ds, & p \geq 2. \end{cases} \tag{63}$$

Note that for $p < 2$, the term $n^{-1/p}$ is dominated by $n^{-1/2}$, so it is omitted from the final upper bound.

The diffusion component.

If $p < 2$, then by condition b) of Theorem 3.1 we have $b(t,x) \equiv 0$, and thus the diffusion component vanishes: **(B)** = 0. It remains to consider the case $p \geq 2$.

Applying the BDG inequality, Lipschitz and Peano assumptions, inequality $(x + y + z)^2 \leq 3(x^2 + y^2 + z^2)$, we get

$$\begin{aligned} \mathbf{(B)}^p &\lesssim \mathbb{E}\left(\int_0^t \left| b(u, X_u) - b(\eta(u), \widetilde{X}_{\eta(u)}) \right|^2 du \right)^{p/2} \\ &\lesssim \mathbb{E}\left(\int_0^t |\mathcal{E}_u|^2 du \right)^{p/2} + \mathbb{E}\left(\int_0^t |\widetilde{X}_u - \widetilde{X}_{\eta(u)}|^2 du \right)^{p/2} \\ &\quad + \mathbb{E}\left(\int_0^t |u-\eta(u)|^{2\gamma} \left(1 + |X_u|\right)^2 du \right)^{p/2}. \end{aligned}$$

In this case we use Minkowski's inequality, which yields

$$\begin{aligned} \mathbf{(B)} &\lesssim \left(\int_0^t \|\mathcal{E}_u\|^2_{L^p(\Omega)} du \right)^{1/2} + \left(\int_0^t \|\widetilde{X}_u - \widetilde{X}_{\eta(u)}\|^2_{L^p(\Omega)} du \right)^{1/2} + n^{-\gamma} \\ &\lesssim \left(\int_0^t f^2(u)du \right)^{1/2} + n^{-\beta} + n^{-1/p} \left(\int_0^t m_p(r)dr \right)^{1/p} + n^{-\gamma} \\ &\lesssim \left(\int_0^t f^2(u)du \right)^{1/2} + n^{-\beta} + n^{-\frac{1}{p}} h^{\frac{\sigma p-\theta_*}{p}} + n^{-\gamma}, \end{aligned} \tag{64}$$

where in the last inequality we used (56) and (60).

The Jump component. We estimate the integrals over small and large balls separately.

By Kunita's or Novikov's (with $a = p$) BDG inequality from (cf. [18, Th.4.20]),

$$\begin{aligned}
\mathbf{(C)}_{sm} &:= \left\| \sup_{s\le t} \left| \int_0^s \int_{B(u,h)} \left(c(u, X_{u-}, z) - c(u, \widetilde{X}_{\eta(u-)}, z) \right) \widetilde{N}(du, dz) \right| \right\|_{L^p(\Omega)} \\
&\lesssim \left(\int_0^t m_p(u) \left\| X_u - \widetilde{X}_{\eta(u)} \right\|^p_{L^p(\Omega)} du \right)^{1/p} \\
&\lesssim \left(\int_0^t m_p(s) f^p(s)\, ds \right)^{1/p} \\
&\quad + \left(\int_0^t m_p(s) \left\| \widetilde{X}_s - \widetilde{X}_{\eta(s)} \right\|^p_{L^p(\Omega)} ds \right)^{1/p}.
\end{aligned}$$

To estimate the second term, we use (56) and inequality $(x + y)^p \lesssim x^p + y^p$:

$$\begin{aligned}
\int_0^t m_p(s) \|\widetilde{X}_s - \widetilde{X}_{\eta(s)}\|^p_{L^p(\Omega)} ds \lesssim n^{-p\beta} \int_0^t m_p(s)\, ds \\
+ \int_0^t m_p(s) \int_{(s-\Delta)^+}^s m_p(u)\, du\, ds.
\end{aligned}$$

By (60), the first term is estimated from above by a term of order $n^{-p\beta} h^{p\sigma - \theta_*}$. For the second term we use (59):

$$I_\Delta(t) := \int_0^t m_p(s) \int_{(s-\Delta)^+}^s m_p(u)\, du\, ds \lesssim h^{2(\sigma p - \theta_*)} \int_0^t s^{-\theta_*} \int_{(s-\Delta)^+}^s u^{-\theta_*}\, du\, ds.$$

Split the integral on the right-hand side into 3 intervals: $s \in (0, \Delta]$, $s \in (\Delta, 2\Delta]$ and $s \in (2\Delta, t]$.

1. For $s \in (0, \Delta]$, the inner integral equals $\int_0^s u^{-\theta_*}\, du = \frac{s^{1-\theta_*}}{1-\theta_*}$, hence

$$\int_0^\Delta s^{-\theta_*} \int_0^s u^{-\theta_*}\, du\, ds = \frac{1}{1-\theta_*} \int_0^\Delta s^{1-2\theta_*}\, ds \lesssim \Delta^{2-2\theta_*}.$$

2. For $s \in (\Delta, 2\Delta]$, we have $s \le 2\Delta$, yielding

$$\int_{s-\Delta}^s u^{-\theta_*}\, du \le \int_0^{2\Delta} u^{-\theta_*}\, du = \frac{(2\Delta)^{1-\theta_*}}{1-\theta_*}.$$

Thus,

$$\int_\Delta^{2\Delta} s^{-\theta_*} \int_{s-\Delta}^s u^{-\theta_*}\, du\, ds \lesssim \Delta^{1-\theta_*} \int_\Delta^{2\Delta} s^{-\theta_*}\, ds \lesssim \Delta^{2-2\theta_*}.$$

3. For $s \in (2\Delta, t]$, we have by the mean value theorem

$$\int_{2\Delta}^t s^{-\theta_*} \int_{s-\Delta}^s u^{-\theta_*}\, du ds \lesssim \int_{2\Delta}^t \Delta s^{-2\theta_*}\, ds.$$

We evaluate this integral by considering different cases for the exponent:

- **Case $\theta_* < \frac{1}{2}$:**

$$\int_{2\Delta}^{t} s^{-2\theta_*}\,ds = \frac{t^{1-2\theta_*} - (2\Delta)^{1-2\theta_*}}{1-2\theta_*} \lesssim 1.$$

- **Case $\theta_* = \frac{1}{2}$:**

$$\int_{2\Delta}^{t} s^{-1}\,ds = \ln(t) - \ln(2\Delta) \lesssim \ln(1/\Delta).$$

- **Case $\theta_* > \frac{1}{2}$:**

$$\int_{2\Delta}^{t} s^{-2\theta_*}\,ds = \frac{t^{1-2\theta_*} - (2\Delta)^{1-2\theta_*}}{1-2\theta_*} \lesssim \Delta^{1-2\theta_*}.$$

Combining all the cases together, we arrive at the final bound:

$$I_\Delta(t) \lesssim \Delta^{\kappa} h^{2(\sigma p-\theta_*)}(1 + \mathbb{1}_{\{\theta_*=\frac{1}{2}\}}|\ln\Delta|).$$

Thus,

$$\mathbf{(C)}_{sm} \lesssim \left(\int_0^t m_p(s) f^p(s)\,ds\right)^{1/p} + n^{-\beta} + n^{-\frac{\kappa}{p}} h^{\frac{2(\sigma p-\theta_*)}{p}}(1 + \mathbb{1}_{\{\theta_*=\frac{1}{2}\}}|\ln\Delta|). \quad (65)$$

Let us estimate now the large jump part

$$\mathbf{(C)}_{lg} := \left\|\sup_{s\le t}\left|\int_0^s \int_{B^c(u,h)} \left(c(u, X_{u-}, z) - c(u, \widetilde{X}_{\eta(u-)}, z)\right) \widetilde{N}(du, dz)\right|\right\|_{L^p(\Omega)}.$$

For the large-jump part, by (12), (15), (14), and Kunita's or Novikov's BDG inequality,

$$\begin{aligned}\mathbf{(C)}_{\mathrm{lg}} &\lesssim \left(\int_0^t M_{p,h}(u)\left\|X_u - \widetilde{X}_{\eta(u)}\right\|_{L^p(\Omega)}^p du\right)^{1/p}\\ &\lesssim \left(\int_0^t M_{p,h}(s) f^p(s)\,ds\right)^{1/p} + \left(\int_0^t M_{p,h}(s)\left\|\widetilde{X}_s - \widetilde{X}_{\eta(s)}\right\|_{L^p(\Omega)}^p ds\right)^{1/p}.\end{aligned}$$

Using (56), inequality $(x+y)^p \lesssim x^p + y^p$ and (14), we get

$$\begin{aligned}\int_0^t M_{p,h}(s)\left\|\widetilde{X}_s - \widetilde{X}_{\eta(s)}\right\|_{L^p(\Omega)}^p ds &\lesssim n^{-p\beta}\int_0^t M_{p,h}(s)\,ds\\ &\quad + \int_0^t M_{p,h}(s)\int_{(s-\Delta)^+}^{s} m_p(u)\,du\,ds\\ &\lesssim n^{-p\beta} + \left(\int_0^t M_{p,h}^{\zeta}(s)ds\right)^{\frac{1}{\zeta}}\\ &\quad \cdot \left(\int_0^t \left(\int_{(s-\Delta)^+}^{s} m_p(u)\,du\right)^{\frac{\zeta}{\zeta-1}} ds\right)^{\frac{\zeta-1}{\zeta}}.\end{aligned}$$

where we used (60) and the assumption that $M_{p,h} \in L^{\zeta}([0,T])$ for $\zeta > 1$ (cf. (14)) with $\theta_* < \frac{\zeta-1}{\zeta}$.

Therefore,

$$\mathbf{(C)}_{\mathrm{lg}} \lesssim \left(\int_0^t M_{p,h}(s) f^p(s)\, ds\right)^{1/p} + n^{-\beta} + n^{-1/p} h^{\frac{p\sigma-\theta_*}{p}}.$$

For $p < 2$, the term $n^{-1/p} h^{\frac{p\sigma-\theta_*}{p}}$ is dominated by $n^{-1/2}$ since $1/p > 1/2$ and $h \in (0, h_0]$. For $p \geq 2$, this term is kept explicitly, in agreement with the definition of $\mathcal{R}_p(n,h)$ in (27).

Combining the bounds for $\mathbf{(C)}_{\mathrm{sm}}$ and $\mathbf{(C)}_{\mathrm{lg}}$, we obtain

$$\begin{aligned}\mathbf{(C)} \lesssim &\left(\int_0^t (m_p(s) + M_{p,h}(s))\, f^p(s)\, ds\right)^{1/p} \\ &+ \begin{cases} n^{-1/2} + n^{-\kappa/p} h^{\frac{2(\sigma p-\theta_*)}{p}} \left(1 + \mathbb{1}_{\{\theta_*=\frac{1}{2}\}} |\ln \Delta|\right), & p < 2, \\ n^{-1/2} + n^{-1/p} h^{\frac{p\sigma-\theta_*}{p}} & \\ \quad + n^{-\kappa/p} h^{\frac{2(\sigma p-\theta_*)}{p}} \left(1 + \mathbb{1}_{\{\theta_*=\frac{1}{2}\}} |\ln \Delta|\right), & p \geq 2. \end{cases}\end{aligned} \tag{66}$$

Gronwall's inequality. We add all three components **(A)**, **(B)** and **(C)**.

From (63), the above estimate of **(B)**, and (66), we obtain an inequality of the form required by Theorem B.1:

$$\begin{aligned} f(t) \lesssim &\int_0^t f(s)\, ds + \mathbb{1}_{\{p\geq 2\}} \left(\int_0^t f^2(s)\, ds\right)^{1/2} + \left(\int_0^t k(s)\, f^p(s)\, ds\right)^{1/p} \\ &+ n^{-\beta} + \mathfrak{r}_p(n,h), \end{aligned}$$

where $\mathfrak{r}_p(n,h)$ corresponds to the remainder terms defined in Lemma A.7, and $k(s) := m_p(s) + M_{p,h}(s)$.

Applying the extended Gronwall lemma (Theorem B.1) yields the explicit bound (53) in Lemma A.7. The simplified convergence rate in Corollary A.8 then follows by choosing h sufficiently small. □

B Auxiliary theorems

Theorem B.1 (Extended Gronwall Lemma [3, Lem.A.1]). *Let $f, \ell : [0,T] \to \mathbb{R}_+$ be non-decreasing functions and $g, h, k \in L^1([0,T], \mathbb{R}_+)$. If for some $p > 1$, $\forall t \in [0,T]$*

$$f(t) \leq \int_0^t g(s) f(s)\, ds + \left(\int_0^t h(s) f^2(s)\, ds\right)^{\frac{1}{2}} + \left(\int_0^t k(s) f^p(s)\, ds\right)^{\frac{1}{p}} + \ell(t),$$

then

$$f(t) \leq 2\, p\, \ell(t) \exp\left(\int_0^t \left(2pg(s) + 2ph(s) + k(s)\right) ds\right).$$

Acknowledgment

The authors are very grateful to the anonymous referees and the chief editor Prof. Yulia Mishura for careful reading and the remarks, which helped us to improve the paper.

References

[1] Asmussen, S.r., Rosiński, J.: Approximations of small jumps of Lévy processes with a view towards simulation. J. Appl. Probab. **38**(2), 482–493 (2001). https://doi.org/https://doi.org/10.1017/s0021900200019987. MR1834755

[2] Bingham, N.H., Goldie, C.M., Teugels, J.L.: Regular Variation. Encyclopedia of Mathematics and Its Applications, vol. 27, p. 491. Cambridge University Press, Cambridge (1987). https://doi.org/https://doi.org/10.1017/CBO9780511721434. https://doi.org/10.1017/CBO9780511721434. MR898871

[3] Bossy, M., Maurer, P.: On the ε-Euler-Maruyama scheme for time inhomogeneous jump-driven SDEs. Stoch. Process. Appl. **190**, Paper No. 104747, 34 pp. (2025). https://doi.org/https://doi.org/10.1016/j.spa.2025.104747. MR4943239

[4] Breton, J.-C., Privault, N.: Integrability and regularity of the flow of stochastic differential equations with jumps. Teor. Veroâtn. Primen. **65**(1), 103–125 (2020). https://doi.org/https://doi.org/10.4213/tvp5291. MR4061867

[5] Butkovsky, O., Dareiotis, K., Gerencsér, M.: Strong Rate of Convergence of the Euler Scheme for SDEs with Irregular Drift Driven by Lévy Noise (2024). https://arxiv.org/abs/2204.12926. MR4982003. https://doi.org/10.1214/24-aihp1506

[6] Çinlar, E.: Introduction to Stochastic Processes, p. 402. Prentice-Hall, Inc., Englewood Cliffs, NJ (1975). MR380912

[7] Fournier, N.: Simulation and approximation of Lévy-driven stochastic differential equations. ESAIM, Probab. Stat. **15**, 233–248 (2011). https://doi.org/https://doi.org/10.1051/ps/2009017. MR2870514

[8] Ikeda, N., Watanabe, S.: Stochastic Differential Equations and Diffusion Processes, 2nd edn. North-Holland Mathematical Library, vol. 24, p. 555. North-Holland Publishing Co., Amsterdam; Kodansha, Ltd., Tokyo (1989). MR1011252

[9] Ivanenko, D., Knopova, V., Platonov, D.: On approximation of some Lévy processes. Austrian J. Stat. **54**(1), 177–199 (2025). https://doi.org/https://doi.org/10.17713/ajs.v54i1.1991

[10] Jacod, J.: The Euler scheme for Lévy driven stochastic differential equations: limit theorems. Ann. Probab. **32**(3A), 1830–1872 (2004). https://doi.org/https://doi.org/10.1214/009117904000000667. MR2073179

[11] Knopova, V.: Compound kernel estimates for the transition probability density of a Lévy process in $\mathbb{R}^n$. Teor. Imovir. Mat. Stat. **89**, 51–63 (2013). https://doi.org/https://doi.org/10.1090/s0094-9000-2015-00935-2. MR3235175

[12] Knopova, V., Kulik, A.: Intrinsic small time estimates for distribution densities of Lévy processes. Random Oper. Stoch. Equ. **21**(4), 321–344 (2013). https://doi.org/https://doi.org/10.1515/rose-2013-0015. MR3139314

[13] Knopova, V., Kulik, A.: Parametrix construction of the transition probability density of the solution to an SDE driven by α-stable noise. Ann. Inst. Henri Poincaré Probab. Stat. **54**(1), 100–140 (2018). https://doi.org/https://doi.org/10.1214/16-AIHP796. MR3765882

[14] Knopova, V., Kulik, A., Schilling, R.L.: Construction and heat kernel estimates of general stable-like Markov processes. Diss. Math. **569**, 86 (2021). https://doi.org/https://doi.org/10.4064/dm824-8-2021. MR4361582

[15] Kohatsu-Higa, A., Tankov, P.: Jump-adapted discretization schemes for Lévy-driven SDEs. Stoch. Process. Appl. **120**(11), 2258–2285 (2010). https://doi.org/https://doi.org/10.1016/j.spa.2010.07.001. MR2684745

[16] Kühn, F.: Existence and estimates of moments for Lévy–type processes. Stoch. Process. Appl. **127**(3), 1018–1041 (2017). https://doi.org/https://doi.org/10.1016/j.spa.2016.07.008. MR3605719

[17] Kühn, F., Schilling, R.L.: Strong convergence of the Euler-Maruyama approximation for a class of Lévy-driven SDEs. Stoch. Process. Appl. **129**(8), 2654–2680 (2019). https://doi.org/https://doi.org/10.1016/j.spa.2018.07.018. MR3980140

[18] Kühn, F., Schilling, R.L.: Maximal inequalities and some applications. Probab. Surv. **20**, 382–485 (2023). https://doi.org/https://doi.org/10.1214/23-ps17. MR4568704

[19] Lewis, P.A.W., Shedler, G.S.: Simulation of nonhomogeneous Poisson processes by thinning. Nav. Res. Logist. Q. **26**(3), 403–413 (1979). https://doi.org/https://doi.org/10.1002/nav.3800260304. MR546120

[20] Li, Y., Zhao, G.: Euler-Maruyama scheme for SDE driven by Lévy process with Hölder drift. Stat. Probab. Lett. **215**, Paper No. 110220, 6 pp. (2024). https://doi.org/https://doi.org/10.1016/j.spl.2024.110220. MR4782995

[21] Menoukeu Pamen, O., Taguchi, D.: Strong rate of convergence for the Euler-Maruyama approximation of SDEs with Hölder continuous drift coefficient. Stoch. Process. Appl. **127**(8), 2542–2559 (2017). https://doi.org/https://doi.org/10.1016/j.spa.2016.11.008. MR3660882

[22] Mikulevičius, R., Xu, F.: On the rate of convergence of strong Euler approximation for SDEs driven by Levy processes. Stochastics **90**(4), 569–604 (2018). https://doi.org/https://doi.org/10.1080/17442508.2017.1381095. MR3784978

[23] Orsingher, E., Ricciuti, C., Toaldo, B.: Time-inhomogeneous jump processes and variable order operators. Potential Anal. **45**(3), 435–461 (2016). https://doi.org/https://doi.org/10.1007/s11118-016-9551-4. MR3554398

[24] Platen, E.: An approximation method for a class of Itô processes with jump component. Liet. Mat. Rink. **22**(2), 124–136 (1982). MR659025

[25] Platen, E., Bruti-Liberati, N.: Numerical Solution of Stochastic Differential Equations with Jumps in Finance. Stochastic Modelling and Applied Probability, vol. 64, p. 856. Springer (2010). https://doi.org/https://doi.org/10.1007/978-3-642-13694-8. https://doi.org/10.1007/978-3-642-13694-8. MR2723480

[26] Protter, P., Talay, D.: The Euler scheme for Lévy driven stochastic differential equations. Ann. Probab. **25**(1), 393–423 (1997). https://doi.org/https://doi.org/10.1214/aop/1024404293. MR1428514

[27] Pruitt, W.E.: General one-sided laws of the iterated logarithm. Ann. Probab. **9**(1), 1–48 (1981). https://doi.org/https://doi.org/10.1214/aop/1176994508. MR606797